

Maximal unitarity for the four-mass double boxHenrik Johansson,^{1,*} David A. Kosower,^{2,†} and Kasper J. Larsen^{3,‡}¹*Theory Group, Physics Department, CERN, CH-1211 Geneva 23, Switzerland*²*Institut de Physique Théorique, CEA-Saclay, F-91191 Gif-sur-Yvette cedex, France*³*Nikhef, Theory Group, Science Park 105, NL-1098 XG Amsterdam, Netherlands*

(Received 15 January 2014; published 11 June 2014)

We extend the maximal-unitarity formalism at two loops to double-box integrals with four massive external legs. These are relevant for higher-point processes, as well as for heavy vector rescattering, $VV \rightarrow VV$. In this formalism, the two-loop amplitude is expanded over a basis of integrals. We obtain formulas for the coefficients of the double-box integrals, expressing them as products of tree-level amplitudes integrated over specific complex multidimensional contours. The contours are subject to the consistency condition that integrals over them annihilate any integrand whose integral over real Minkowski space vanishes. These include integrals over parity-odd integrands and total derivatives arising from integration-by-parts (IBP) identities. We find that, unlike the zero- through three-mass cases, the IBP identities impose no constraints on the contours in the four-mass case. We also discuss the algebraic varieties connected with various double-box integrals and show how discrete symmetries of these varieties largely determine the constraints.

DOI: 10.1103/PhysRevD.89.125010

PACS numbers: 12.38.Bx, 12.38.-t, 11.15.-q

I. INTRODUCTION

Last year's discovery [1,2] by the ATLAS and CMS Collaborations of a Higgs-like boson completes the particle content of the Standard Model. Coupled with the absence to date of direct signals of physics beyond the Standard Model, the discovery points towards an important role for precision measurements in determining the scale of new physics beyond the Standard Model.

Theoretical calculations at the LHC, whether for signals or backgrounds, begin with the tree-level amplitudes required for leading-order (LO) calculations in perturbative quantum chromodynamics (QCD). Because the strong coupling α_s is relatively large and runs quickly, LO predictions suffer from strong dependence on the unphysical renormalization and factorization scales and are thus not quantitatively reliable. Next-to-leading order (NLO) is the lowest order in perturbation theory which offers quantitatively reliable predictions. These calculations require one-loop amplitudes in addition to tree-level amplitudes with higher multiplicity. Recent years have seen major advances in NLO calculations, especially for processes with several jets in the final state [3–9]. While the uncertainty left by scale variation cannot be quantified in the same fashion as statistical uncertainties, experience shows that it is of $\mathcal{O}(10\%–15\%)$.

As combined experimental uncertainties in future measurements push below this level, a comparison with theoretical calculations will require pushing on to

next-to-next-to-leading-order (NNLO) accuracy. Such studies will require computation of two-loop amplitudes. These computations form the next frontier of precision QCD calculations. The only existing fully exclusive NNLO jet calculations to date are for three-jet production in electron-positron annihilation [10]. These calculations have been used to determine α_s to 1% accuracy from jet data at LEP [11]. This extraction is competitive with other determinations. Beyond their use in seeking deviations in precision experimental data from Standard-Model predictions, NNLO calculations will also be useful at the LHC for improving our understanding of scale stability in multiscale processes such as $W +$ multijet production, as well as for providing honest theoretical uncertainty estimates for NLO calculations.

The unitarity method [12–29] has made many previously inaccessible one-loop calculations feasible. Of particular note are processes with many partons in the final state. The most recent development, applying generalized unitarity, allows the method to be applied either analytically or purely numerically [30–40]. The numerical formalisms underlie recent software libraries and programs that have been applied to LHC phenomenology. In this approach, the one-loop amplitude in QCD is written as a sum over a set of basis integrals, with coefficients that are rational in external spinors:

$$\text{Amplitude} = \sum_{j \in \text{Basis}} \text{coefficient}_j \times \text{Integral}_j + \text{Rational}. \quad (1.1)$$

The integral basis for amplitudes with massless internal lines contains box, triangle, and bubble integrals in addition

*Henrik.Johansson@cern.ch

†David.Kosower@cea.fr

‡Kasper.Larsen@nikhef.nl

to purely rational terms [dropping all terms of $\mathcal{O}(\epsilon)$ in the dimensional regulator]. The coefficients are calculated from products of tree amplitudes, typically by performing contour integrals via discrete Fourier projection. In the Ossola-Papadopoulos-Pittau (OPP) approach [21], this decomposition is carried out at the integrand level rather than at the level of integrated expressions.

Higher-loop amplitudes can also be written in the form given in Eq. (1.1). As at one loop, one can carry out such a decomposition at the level of the integrand. This generalization of the OPP approach has been pursued by Mastrolia and Ossola [41] and collaborators, and also by Badger, Frellesvig, and Zhang [42]. The reader should consult Refs. [43–49] for further developments within this approach. Arkani-Hamed and collaborators have developed an integrand-level approach [50–55] specialized to planar contributions to the $\mathcal{N} = 4$ supersymmetric theory, but to all loop orders.

Within the unitarity method applied at the level of integrated expressions, one can distinguish two basic approaches. In a “minimal” application of generalized unitarity, used in a number of prior applications and currently pursued by Feng and Huang [56], one cuts just enough propagators to break apart a higher-loop amplitude into a product of disconnected tree amplitudes. Each cut is then a product of tree amplitudes, but because not all possible propagators are cut, each generalized cut will correspond to several integrals, and algebra will be required to isolate specific integrals and their coefficients. This approach does not require a predetermined general basis of integrals; it can be determined in the course of a specific calculation. A number of calculations have been done this way, primarily in the $\mathcal{N} = 4$ supersymmetric gauge theory [57–64], but including several four-point calculations in QCD and supersymmetric theories with less-than-maximal supersymmetry [65–71]. Furthermore, a number of recent multiloop calculations in maximally supersymmetric gauge and gravity theories have used maximal cuts [72–78], without complete localization of integrands.

We will use a more intensive form or “maximal” form of generalized unitarity. In this approach, one cuts as many propagators as possible and further seeks to fully localize integrands onto global poles to the extent possible. In principle, this allows one to isolate individual integrals on the right-hand side of the higher-loop analog of Eq. (1.1). In previous papers [79,80], we showed how to extract the coefficients of double-box master integrals using multidimensional contours around global poles. In this paper, we recast this operation as applying *generalized discontinuity operators* (GDOs). Each GDO corresponds to integrating the integrand of an amplitude or an integral along a specified linear combination of multidimensional contours around global poles. The GDOs generalize the operation of cutting via the Cutkosky-rule replacement of propagators by on-shell delta functions.

Some of the contour integrations in a GDO put internal lines on shell, equivalent to cutting propagators [81]. This integration will typically yield a Jacobian giving rise to poles in the remaining degrees of freedom. In the case of the double box, the Jacobian allows one to fully localize the remaining degrees of freedom through additional multidimensional contour integrals. The integrand is then fully localized at one of a set of global poles. We call these additional degrees of freedom “localization variables.” We include these additional dimensions of contours in the definition of the GDO. This maximal-unitarity approach may be viewed as a generalization to two loops of the work of Britto, Cachazo, and Feng [16] and of Forde [23].

The GDOs are constructed so that each one selects a specific master integral:

$$\text{GenDisc}_i(\text{Integral}_j) = \delta_{ij}. \quad (1.2)$$

Applying it to Eq. (1.1) then gives us an expression for the corresponding coefficient:

$$\text{coefficient}_j = \text{GenDisc}_j(\text{Amplitude}). \quad (1.3)$$

The right-hand side will have the form of explicit contour integrals over localization variables of a product of tree amplitudes; schematically,

$$\text{coefficient}_j = \oint_{\Gamma_j} dz_i \prod A^{\text{tree}}(z_i). \quad (1.4)$$

The weights with which the contours Γ_j surround the different global poles are determined by a set of consistency equations. These equations require that integrals vanishing over the Minkowski slice of complexified loop-momentum space are also annihilated by the GDOs, vanishing on the particular combinations of contours in each and every GDO.

In this paper, we continue the maximal-unitarity approach of Refs. [79,80], relying on the global-pole analysis [82] of Caron-Huot and one of the present authors. At higher loops, the coefficients of the basis integrals are no longer rational functions of the external spinors alone but will in general depend explicitly on the dimensional regulator ϵ . We consider GDOs operating only on the four-dimensional components of the loop momenta and accordingly extract only the leading terms, ϵ -independent terms. GDOs operating on the full D -dimensional loop momenta would be required to extract the remaining terms and could presumably be used to obtain the rational terms in Eq. (1.1) as well.

At two loops and beyond, the number of master integrals for a given topology will depend on the number and arrangement of external masses [83]. (See also recent work on a different organization of higher-loop integrals [84–86].) In previous papers, we have considered double

boxes with no external masses [79] or with one, two, or three external masses [80]. In this article, we extend the GDO construction to planar double boxes with four external masses. We consider both the general case with unequal masses and one special case with pairs of equal masses. In the general case, there are four master integrals; in the special case with an extra reflection symmetry, three. Sjøgaard [87] has constructed GDOs for the nonplanar massless double box.

As in previous work, we ensure the consistency of the GDOs by requiring that they yield a vanishing result when applied to vanishing integrals. For the four-mass double box, it turns out that nontrivial constraints arise only from parity-odd integrands; integration-by-parts (IBP) identities [88–95] give no additional constraints. The symmetry requirement for the special equal-mass case must also be imposed explicitly and, unlike fewer-mass cases, does not emerge automatically from IBP equations. We consider only two-loop master integrals with massless internal lines. We will not consider the generalization to massive internal lines; but so long as there are sufficient massless internal lines to have at least one chiral vertex, the integrand should still have global poles, and we should expect the approach described here to generalize smoothly.

This paper is organized as follows. In Sec. II, we present the parametrization of loop momenta we use for derivations. In Sec. III, we discuss the maximal-cut equations for the four-mass double box along with the global poles and derive the GDOs for the four master integrals. In Sec. IV, we discuss constraint equations and their symmetries for all double boxes from an algebraic-geometry point of view. We make some concluding remarks in Sec. V.

II. LOOP-MOMENTUM PARAMETRIZATION

We take over the same loop-momentum parametrization used in Ref. [80]. This parametrization makes use of spinors defined for massive external legs. Such spinors correspond to massless four-dimensional momenta, which we obtain using “mutually projected” kinematics. This construction was previously used in the work of OPP [21] and Forde [23] to extract triangle and bubble coefficients at one loop.

For a given pair of external four-momenta (k_i, k_j) , we require the mutually projected momenta to satisfy

$$k_i^{b,\mu} = k_i^\mu - \frac{k_i^2}{2k_i \cdot k_j^b} k_j^{b,\mu}, \quad k_j^{b,\mu} = k_j^\mu - \frac{k_j^2}{2k_j \cdot k_i^b} k_i^{b,\mu}. \quad (2.1)$$

By construction, k_i^b and k_j^b are massless momenta. Next, define

$$\rho_{ij} \equiv \frac{k_i^2}{2k_i \cdot k_j^b}. \quad (2.2)$$

We note that

$$k_i \cdot k_j^b = k_i^b \cdot k_j = k_i^b \cdot k_j^b \quad (2.3)$$

and define

$$\gamma_{ij} \equiv 2k_i^b \cdot k_j^b, \quad (2.4)$$

so that $\rho_{ij} = k_i^2/\gamma_{ij}$. After using Eq. (2.1), we obtain a quadratic equation for γ_{ij} ; its two solutions are

$$\gamma_{ij}^\pm = k_i \cdot k_j \pm [(k_i \cdot k_j)^2 - k_i^2 k_j^2]^{1/2}. \quad (2.5)$$

If either momentum in the pair (k_i, k_j) is massless, only one solution survives. Equation (2.3) then gives us $\gamma_{ij} = 2k_i \cdot k_j$. Inverting Eq. (2.1), we obtain the massless momenta

$$k_i^{b,\mu} = (1 - \rho_{ij}\rho_{ji})^{-1}(k_i^\mu - \rho_{ij}k_j^\mu); \quad (2.6)$$

swap $i \leftrightarrow j$ to obtain $k_j^{b,\mu}$. In this paper we work with two mutually projected pairs: (k_1, k_2) and (k_3, k_4) . This choice defines a set of “projected” massless momenta $k_i^{b,\mu}$, $i = 1, \dots, 4$, in terms of the external momenta, k_i , and the sign choices in γ_{12}^\pm and γ_{34}^\pm .

With the projected momenta, we adopt the following parametrization for the double-box loop momenta as depicted in Fig. 1:

$$e_1^\mu = \frac{1}{2} \langle \lambda_1 | \gamma^\mu | \tilde{\lambda}'_1 \rangle + \zeta_1 \eta_1^\mu, \quad e_2^\mu = \frac{1}{2} \langle \lambda_2 | \gamma^\mu | \tilde{\lambda}'_2 \rangle + \zeta_2 \eta_2^\mu, \quad (2.7)$$

where ζ_i are complex numbers, and the η_i are null vectors satisfying $\tilde{\eta}_1 |\lambda_1\rangle \neq 0 \neq \tilde{\eta}_1 |\tilde{\lambda}'_1\rangle$ and $\tilde{\eta}_2 |\lambda_2\rangle \neq 0 \neq \tilde{\eta}_2 |\tilde{\lambda}'_2\rangle$. We introduce the ζ_i in order to compute Jacobian factors arising from the change of variables in the double-box integral. To obtain on-shell momenta, we subsequently set $\zeta_i = 0$.

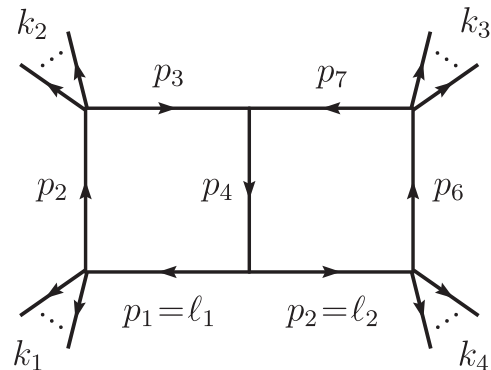


FIG. 1. The double-box integral.

We write the various loop spinors in Eq. (2.7) in terms of the spinors corresponding to (k_1^b, k_2^b) for ℓ_1 and the spinors corresponding to (k_3^b, k_4^b) for ℓ_2 :

$$\begin{aligned} |\lambda_1\rangle &= \xi_1 |1^b\rangle + \xi_2 \frac{\langle 4^b 1^b \rangle}{\langle 4^b 2^b \rangle} |2^b\rangle, & |\tilde{\lambda}'_1\rangle &= \xi'_1 |1^b\rangle + \xi'_2 \frac{[4^b 1^b]}{[4^b 2^b]} |2^b\rangle, \\ |\lambda_2\rangle &= \xi_3 \frac{\langle 1^b 4^b \rangle}{\langle 1^b 3^b \rangle} |3^b\rangle + \xi_4 |4^b\rangle, & |\tilde{\lambda}'_2\rangle &= \xi'_3 \frac{[1^b 4^b]}{[1^b 3^b]} |3^b\rangle + \xi'_4 |4^b\rangle, \end{aligned} \quad (2.8)$$

where the external spinors are defined via $k_i^{b,\mu} = \langle i^b | \gamma^\mu | i^b \rangle / 2$. Without loss of generality, we can set two of the complex parameters to unity, $\xi_1 = \xi_4 = 1$, as we will do throughout the paper.

Moreover, similarly to Ref. [80], we define the following quantities:

$$\begin{aligned} \bar{\xi}'_1 &\equiv \frac{\gamma_{12} s_{12} - (\gamma_{12} + m_2^2) m_1^2}{\gamma_{12}^2 - m_1^2 m_2^2}, \\ \bar{\xi}'_2 &\equiv -\frac{m_1^2 (s_{12} - \gamma_{12} - m_1^2) k_2^b \cdot k_4^b}{(\gamma_{12}^2 - m_1^2 m_2^2) k_1^b \cdot k_4^b}, \\ \bar{\xi}'_3 &\equiv -\frac{m_4^2 (s_{34} - \gamma_{34} - m_4^2) k_1^b \cdot k_3^b}{(\gamma_{34}^2 - m_3^2 m_4^2) k_1^b \cdot k_4^b}, \\ \bar{\xi}'_4 &\equiv \frac{\gamma_{34} s_{34} - (\gamma_{34} + m_3^2) m_4^2}{\gamma_{34}^2 - m_3^2 m_4^2}, \end{aligned} \quad (2.9)$$

$$\tau \equiv \frac{\langle 1^b 4^b \rangle \langle 2^b 3^b \rangle}{\langle 2^b 4^b \rangle \langle 1^b 3^b \rangle} = \frac{[1^b 4^b][2^b 3^b]}{[2^b 4^b][1^b 3^b]}, \quad (2.10)$$

where m_i are the masses of the external momenta, $m_i^2 = k_i^2$. In addition, we will make use of the following quantities not needed in Ref. [80]:

$$\Delta \equiv ((\bar{\xi}'_1 + \bar{\xi}'_2) \bar{\xi}'_4 - (\bar{\xi}'_1 + \tau^2 \bar{\xi}'_2) \bar{\xi}'_3)^2 - 4 \bar{\xi}'_1 \bar{\xi}'_2 (\tau \bar{\xi}'_3 - \bar{\xi}'_4)^2, \quad (2.11)$$

$$z_{\pm} \equiv \frac{1}{2 \bar{\xi}'_1 (\tau \bar{\xi}'_3 - \bar{\xi}'_4)} ((\bar{\xi}'_1 + \bar{\xi}'_2) \bar{\xi}'_4 - (\bar{\xi}'_1 + \tau^2 \bar{\xi}'_2) \bar{\xi}'_3 \pm \sqrt{\Delta}), \quad (2.12)$$

$$\gamma_* \equiv \frac{\gamma_{12} \gamma_{34}}{32 k_1^b \cdot k_4^b (\gamma_{12}^2 - m_1^2 m_2^2) (\gamma_{34}^2 - m_3^2 m_4^2)}. \quad (2.13)$$

III. MAXIMAL CUTS OF DOUBLE-BOX INTEGRALS

Our aim is to determine the coefficients of the double-box master integrals that appear in the basis expansion (1.1) of a two-loop quantity that may either be an amplitude, form factor, or correlator. Without loss of generality, we refer to the two-loop quantity as an amplitude. The

double-box integral topology is illustrated in Fig. 1 and defines the internal momenta p_j . The integral is defined in dimensional regularization with $D = 4 - 2\epsilon$ as

$$P_{2,2}^{**}[\Phi] \equiv \int_{\mathbb{R}^D \times \mathbb{R}^D} \frac{d^D \ell_1}{(2\pi)^D} \frac{d^D \ell_2}{(2\pi)^D} \frac{\Phi(k_1, k_2, k_3; \ell_1, \ell_2)}{\prod_{j=1}^7 p_j^2}, \quad (3.1)$$

where Φ denotes an arbitrary polynomial in the external and internal momenta. We refer to it as a numerator insertion. At one loop, all numerator insertions can be expressed as linear combinations of propagator denominators, external invariants, and parity-odd functions which vanish upon integration; but this is no longer true at two loops and beyond. At higher loops, some polynomials Φ are irreducible. Integrals with certain irreducible-numerator insertions can be related to others using IBP identities, but in general several will remain as master integrals.

We seek formulas for the double-box coefficients to leading order in the dimensional regulator ϵ in terms of purely tree-level input. We begin by cutting all double-box propagators on both sides of Eq. (1.1). This immediately eliminates all integrals with fewer than seven propagators, or with a different topology, as cutting an absent propagator yields zero.

Heuristically, we may imagine using the Cutkosky rules and simply replacing the cut propagators by on-shell delta functions. On the left-hand side of the equation, we would then obtain

$$A^{(2)}|_{\text{cut}} = (2\pi i)^7 \int \frac{d^4 \ell_1}{(2\pi)^4} \frac{d^4 \ell_2}{(2\pi)^4} \prod_{j=1}^7 \delta(p_j^2) \prod_{v=1}^6 A_{(v)}^{\text{tree}}, \quad (3.2)$$

where $A_{(v)}^{\text{tree}}$ denote the tree processes at each of the six vertices of the diagram in Fig. 1 and p_j denote the momenta flowing through each of the propagators. The cuts have also eliminated any potential infrared divergences, so we can take the four-dimensional limit for the integrand. On the right-hand side of Eq. (1.1), we would obtain a sum over expressions of the form

$$\begin{aligned} &\text{coefficient} \times P_{2,2}^{**}[\Phi]|_{\text{cut}} \\ &= \text{coefficient} \times (2\pi i)^7 \int \frac{d^4 \ell_1}{(2\pi)^4} \frac{d^4 \ell_2}{(2\pi)^4} \prod_{j=1}^7 \delta(p_j^2) \Phi. \end{aligned} \quad (3.3)$$

If we interpret the expressions in Eqs. (3.2) and (3.3) literally, however, we face a problem. The integrations in these equations receive contributions only from regions of integration space where the loop momenta solve the joint on-shell constraints

$$p_j^2 = 0, \quad j = 1, \dots, 7. \quad (3.4)$$

For generic external momenta, the solutions to these equations are complex. So long as the integrations are over real momenta ($\mathbb{R}^4 \times \mathbb{R}^4$), we simply get zero. Equating the two expressions will yield $0 = 0$, which is true but useless for extracting the coefficient in Eq. (3.3).

Instead of thinking of the loop integrals as integrals over real momenta, we can choose to think of them as integrals in complex momenta, $\ell_i \in \mathbb{C}^4$, taken along contours comprising the real slice, $\text{Im } \ell_i^\mu = 0$. Changing the contour then gives us an alternative way of imposing a delta-function constraint, one that is valid for complex as well as for real solutions.

The utility of reinterpreting delta functions as contour integrals was previously observed in the context of twistor-string amplitudes [96,97] and is also standard in more formal twistor-space expressions [98]. In one dimension, we seek to localize an integral,

$$\int dq \delta(q - q_0) h(q) = h(q_0), \quad (3.5)$$

even if q_0 becomes complex. Cauchy's residue theorem gives us precisely such a localization if we replace $\delta(q - q_0)$ by $\frac{1}{2\pi i} \frac{1}{q - q_0}$ and take the integral to be a contour integral along a small circle centered at q_0 in the complex q plane. Analogously, a product of delta functions can be defined as a multidimensional contour integral,

$$(2\pi i)^n \int dq_1 \dots dq_n h(q_i) \prod_{j=1}^n \delta(q_j - q_{0j}) \\ \stackrel{\text{def}}{=} \int_{T_\varepsilon(q_0)} dq_1 \dots dq_n \frac{h(q_i)}{\prod_{j=1}^n (q_j - q_{0j})}, \quad (3.6)$$

where the contour $T_\varepsilon(q_0)$ is now a torus encircling the simultaneous solution of denominator equations. For the simple form of the denominator here, the contour will be a product of n small circles ($\varepsilon \ll 1$), $T_\varepsilon(q_0) = C_\varepsilon(q_{01}) \times \dots \times C_\varepsilon(q_{0n})$, each centered at q_{0j} . The simultaneous solution of the denominator equations is called a *global pole*. The question of what it means for a torus to encircle a global pole is much more subtle in higher dimensions than for a contour to encircle a point in one complex dimension; but the subtleties will play no role in the present article.

There is one important respect in which the multidimensional contour integrals behave differently from integrals over delta functions, namely the transformation formula for changing variables. Given a holomorphic function $f = (f_1, \dots, f_n): \mathbb{C}^n \rightarrow \mathbb{C}^n$ with an isolated zero¹

¹A function $f = (f_1, \dots, f_n): \mathbb{C}^n \rightarrow \mathbb{C}^n$ is said to have an isolated zero at $a \in \mathbb{C}^n$ iff by choosing a small enough neighborhood U of a one can ensure that it has only a single zero in the neighborhood, so that $f^{-1}(0) \cap U = \{a\}$.

at $a \in \mathbb{C}^n$, the residue at a is computed by performing the integral over a toroidal contour, whose general definition is $T_\varepsilon(a) = \{z \in \mathbb{C}^n : |f_i(z)| = \varepsilon_i, i = 1, \dots, n\}$. This contour integral satisfies the transformation formula

$$\frac{1}{(2\pi i)^n} \int_{T_\varepsilon(a)} \frac{h(z) dz_1 \wedge \dots \wedge dz_n}{f_1(z) \dots f_n(z)} = \frac{h(a)}{\det_{i,j} \frac{\partial f_i}{\partial z_j}}. \quad (3.7)$$

Unlike the conventional formula for a multidimensional real integral over delta functions, it does not involve taking the absolute value of the inverse Jacobian. This ensures that this factor is analytic in any remaining variables on which it depends, so that further contour integrations can be carried out.

We use multidimensional contour integrals to define generalized discontinuity operators. The GDOs for the double box will be eightfold integrals taken over contours that are linear combinations of basis contours. Each basis contour encircles a single global pole, and we will refer to global poles and their encircling contours interchangeably. Applying a GDO means changing the contour of the integration from one over the real slice of $\mathbb{C}^4 \times \mathbb{C}^4$ to one over the GDO's associated contour. We want seven of the eight contour integrations to correspond to the seven on-shell constraints $p_j^2 = 0$; to do so, the contours must ultimately encircle solutions to these constraints. The integrands in Eqs. (3.2) and (3.3) are left unchanged. Imposing the seven constraints leaves one complex degree of freedom. The heptacut constraints thus define a Riemann surface in $\mathbb{C}^4 \times \mathbb{C}^4$. As we will see below, this Riemann surface contains a number of poles. Their presence will allow us to freeze the remaining degree of freedom, by choosing an appropriate contour of integration for the corresponding localization variable. Before discussing the poles, however, we first review the structure of the Riemann surface.

A. Kinematical solutions, Jacobians and global poles

As discussed in Ref. [82], the maximal-cut Riemann surface for the double-box integral is a pinched torus, with the number of pinches equal to twice the number of vertical double-box rungs that attach to an on-shell massless three-point vertex. An on-shell massless three-point vertex is either chiral or antichiral, enforcing a twofold branching of the kinematical parametrization and implying a pinching of the parameter space. A more careful analysis of the kinematical solutions shows that chiral vertices are (anti) correlated across the vertical rungs of the double-box integral. Hence, we classify the different types of pinches by their effect on the vertical rungs.

In previous work [80], we assigned double boxes to one of three classes (a), (b), or (c), according to whether an on-shell massless three-point vertex is connected to (a) the middle rung, (b) the middle rung and one outer rung, or (c)

all three vertical rungs.² We treated the two latter classes in Ref. [80]. Here, we consider class (a), corresponding to the four-mass double box, illustrated in Fig. 1. In this class, the solutions to the heptacut equations (3.4) form a doubly pinched torus, shown in Fig. 2.

Each lobe of the doubly pinched torus corresponds to one of two kinematical solutions \mathcal{S}_1 and \mathcal{S}_2 . In terms of the loop-momentum parametrization of Eq. (2.7), both solutions have $\xi'_1 = \bar{\xi}'_1$, $\xi'_4 = \bar{\xi}'_4$, $\xi_1 = \xi_4 = 1$, and the remaining four variables $(\xi_2, \xi_2', \xi_3, \xi_3')$ take on the following values:

$$\begin{aligned} \mathcal{S}_1: & \left(\frac{\bar{\xi}'_2}{z}, z, -\frac{(z + \bar{\xi}'_1/\tau)\tau\bar{\xi}'_3}{(z + \bar{\xi}'_1)\xi_4}, -\frac{(z + \bar{\xi}'_1)\bar{\xi}'_4}{(z + \bar{\xi}'_1/\tau)\tau} \right), \\ \mathcal{S}_2: & \left(z, \frac{\bar{\xi}'_2}{z}, -\frac{z+1}{\tau z+1}, -\frac{(\tau z+1)\bar{\xi}'_3}{z+1} \right), \end{aligned} \quad (3.8)$$

where the $\bar{\xi}'_i$ are defined in Eq. (2.9). The Jacobian that arises from changing the integration variables of Eq. (3.1) to the ξ_i, ξ'_i, ζ_i in Eqs. (2.7) and (2.8) and subsequently performing seven contour integrals, $\int d^4\ell_1 d^4\ell_2 \prod_{j=1}^7 1/p_j^2 \rightarrow \int dz J_{\mathcal{F}}$, takes the generic form

$$\begin{aligned} J_{\mathcal{F}}(z)|_{\mathcal{S}_i} & \equiv \left(\det_{\mu,i} \frac{\partial \ell_1^\mu}{\partial v_{1,i}} \right) \left(\det_{\nu,j} \frac{\partial \ell_2^\nu}{\partial v_{2,j}} \right) \left(\det_{i,j} \frac{\partial p_i^2}{\partial w_j} \right)^{-1} \\ & = \frac{C_i}{(z - z_{i,1})(z - z_{i,2})}, \end{aligned} \quad (3.9)$$

where in the first equality $v_{j,1} = \zeta_j$, $v_{1,2} = \xi'_1$, $v_{2,2} = \xi'_4$, $v_{1,3} = \xi_2$, $v_{2,3} = \xi_3$, $v_{1,4} = \xi'_2$, and $v_{2,4} = \xi'_3$, and w_j are the seven variables frozen by the contour integrations. In the second equality, $(z_{i,1}, z_{i,2})$ are the local coordinates of the intersection with the neighboring solution(s)

$$\mathcal{S}_i|_{z=z_{i,1}} \in \mathcal{S}_{i-1} \cap \mathcal{S}_i, \quad \mathcal{S}_i|_{z=z_{i,2}} \in \mathcal{S}_i \cap \mathcal{S}_{i+1}. \quad (3.10)$$

More generally, the Jacobian evaluated on a Riemann sphere will always be a product of simple-pole factors associated with the pinching points (also known as nodal points) on the sphere.

As mentioned above, the heptacut of the double-box integral arises from performing seven of the eight contour integrals and yields a Riemann surface given by the solution to the joint on-shell constraints (3.4). We are left with a single complex degree of freedom (or localization variable) z and the freedom to choose a contour for its integration. In order to localize the integrand completely, we should have this last contour encircle a pole in z . As in classes (b) and (c) treated in Ref. [80], such poles can arise from two sources: the Jacobian factor (3.9) or from the

² $P_{2,2}$ or ‘‘flying-squirrel!’’ integrals (in the notation of Ref. [83]), with external legs attached to the middle vertices of the double box, would yield novel classes [82] and are not treated here.

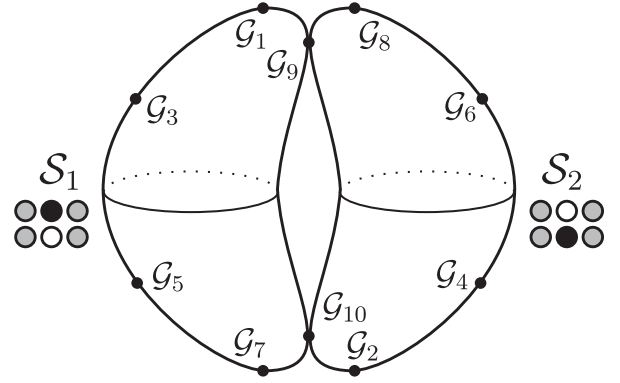


FIG. 2. A representation of the pinched torus solution space for the class (a) heptacut kinematics, showing the two independent solutions \mathcal{S}_i , and the locations of the eight global poles \mathcal{G}_i . The small white, black and gray blobs indicate the pattern of chiral, antichiral and nonchiral kinematics, respectively, at the vertices of a double-box integral. Complex-conjugate pairs of poles are identified by reflection through the center of the torus.

numerator insertions Φ in Eq. (3.1), which introduce an additional dependence on z .

The Jacobian poles are the pinching points $\mathcal{G}_{9,10}$ in Fig. 2. Because these points are shared between different on-shell solutions, one must decide on a convention for the sphere on which the corresponding residue is to be evaluated. We adopt the convention of computing the residue on the sphere located on the anticlockwise side of the Riemann surface. In Fig. 2, for example, the residue at \mathcal{G}_9 should be evaluated on \mathcal{S}_1 ; and the residue at \mathcal{G}_{10} on \mathcal{S}_2 . Furthermore, we choose the orientations on each Riemann sphere such that for any global pole $\mathcal{G}_k \in \mathcal{S}_i \cap \mathcal{S}_j$, the residues evaluated on spheres \mathcal{S}_i and \mathcal{S}_j are equal in magnitude but opposite in sign. That is, for an arbitrary function f of the loop momenta one has

$$\begin{aligned} \text{Res}_{\mathcal{S}_i \cap \mathcal{S}_{i+1}} J_{\mathcal{F}}(z) f(\ell_1(z), \ell_2(z))|_{\mathcal{S}_i} \\ = - \text{Res}_{\mathcal{S}_i \cap \mathcal{S}_{i+1}} J_{\mathcal{F}}(z) f(\ell_1(z), \ell_2(z))|_{\mathcal{S}_{i+1}}, \end{aligned} \quad (3.11)$$

in agreement with the conventions of Refs. [80,82]. Other choices of conventions are possible, but all will lead to the same final expressions for the two-loop integral coefficients.

The class (a) Jacobian, as defined in Eq. (3.9), takes the form

$$J_{\mathcal{F}} = \begin{cases} J_{\mathcal{F}}^{(a,1)} \equiv \frac{\bar{\xi}'_1}{(z - \bar{\xi}'_1 z_+) (z - \bar{\xi}'_1 z_-)}, & \text{for solution } \mathcal{S}_1, \\ J_{\mathcal{F}}^{(a,2)} \equiv \frac{1}{(z - z_+) (z - z_-)}, & \text{for solution } \mathcal{S}_2, \end{cases} \quad (3.12)$$

after the convenient rescaling $J_f \rightarrow \frac{\bar{\xi}'_1(\bar{\xi}'_4 - \tau\bar{\xi}'_3)}{\gamma_*} J_f$, in analogy with Eqs. (4.7) and (4.8) of Ref. [80]. (The rescaling of course leaves the final formulas for integral coefficients unchanged.) Note that $z_+ z_- = \bar{\xi}'_2/\bar{\xi}'_1$.

In addition to the Jacobian poles, we may choose the contour for the remaining degree of freedom (after performing the heptacut) to encircle any of the points on the Riemann surface where a loop momentum becomes infinite. At such points, numerator insertions $\Phi(p_i)$ have a pole in z . We will refer to these points, shown as punctures on the spheres in Fig. 2, as insertion poles. There are eight such poles, so that altogether we have ten global poles which the z contour integral may encircle, located at the following values of $(\xi_2, \bar{\xi}'_2, \xi_3, \bar{\xi}'_3)$:

$$\begin{aligned} \mathcal{G}_1 &: \left(-\frac{\bar{\xi}'_2}{\bar{\xi}'_1}, -\bar{\xi}'_1, \infty, 0 \right), & \mathcal{G}_2 &: (-1, -\bar{\xi}'_2, 0, \infty), \\ \mathcal{G}_3 &: \left(0, \infty, -\frac{\tau\bar{\xi}'_3}{\bar{\xi}'_4}, -\frac{\bar{\xi}'_4}{\tau} \right), & \mathcal{G}_4 &: \left(\infty, 0, -\frac{1}{\tau}, -\tau\bar{\xi}'_3 \right), \\ \mathcal{G}_5 &: \left(-\frac{\tau\bar{\xi}'_2}{\bar{\xi}'_1}, -\frac{\bar{\xi}'_1}{\tau}, 0, \infty \right), & \mathcal{G}_6 &: \left(-\frac{1}{\tau}, -\tau\bar{\xi}'_2, \infty, 0 \right), \\ \mathcal{G}_7 &: \left(\infty, 0, -\frac{\bar{\xi}'_3}{\bar{\xi}'_4}, -\bar{\xi}'_4 \right), & \mathcal{G}_8 &: (0, \infty, -1, -\bar{\xi}'_3), \\ \mathcal{G}_9 &: \left(z_+, \frac{\bar{\xi}'_2}{z_+}, -\frac{(z_+\bar{\xi}'_1 + \tau\bar{\xi}'_2)\bar{\xi}'_3}{(z_+\bar{\xi}'_1 + \bar{\xi}'_2)\bar{\xi}'_4}, -\frac{(z_+\bar{\xi}'_1 + \bar{\xi}'_2)\bar{\xi}'_4}{z_+\bar{\xi}'_1 + \tau\bar{\xi}'_2} \right), \\ \mathcal{G}_{10} &: \left(z_-, \frac{\bar{\xi}'_2}{z_-}, -\frac{1+z_-}{1+\tau z_-}, -\frac{(1+\tau z_-)\bar{\xi}'_3}{1+z_-} \right). \end{aligned} \quad (3.13)$$

In the above labeling, the poles $(\mathcal{G}_{2j-1}, \mathcal{G}_{2j})$, $j = 1, \dots, 7$ form parity-conjugate pairs. Because parity amounts to swapping chiralities $\bullet \longleftrightarrow \circ$, thereby rotating Fig. 2 by an angle π , parity-conjugate pairs always appear antipodally in the figure. We note that at the pinching points $\mathcal{G}_{9,10}$, the loop momentum flowing through the middle rung of the double box becomes soft, $p_4 \rightarrow 0$. At the remaining global poles, either the left or right loop momentum goes to infinity in a particular direction. (See Appendix A for a more detailed discussion.)

Let us denote a contour consisting of a small circle around \mathcal{G}_j by C_j . The set of circles around all of the ten poles in Fig. 2 forms an overcomplete basis of contours for GDOs and equivalently an overcomplete basis for homology. On each sphere we can use the fact that all residues sum to zero to eliminate any one contour C_j in favor of the remaining ones. This is not sufficient, as we must impose additional consistency constraints on the linear combination of contours by which every GDO acts. We discuss these below. Retaining all contours instead of choosing a linearly independent subset does have the advantage of making manifest certain discrete symmetries, clarifying the

structure of the additional consistency constraints. We examine this issue in more detail in Sec. IV.

The truncation to a linearly independent homology basis can be achieved simply by setting the coefficients of certain contours to zero in every GDO. Not all truncations will lead to a valid basis, however; a basis must necessarily contain a contour encircling at least one of the pinching points $\mathcal{G}_{9,10}$. To understand why, consider the sum of all residues on \mathcal{S}_1 plus the sum of all residues on \mathcal{S}_2 . Both sums are zero by Cauchy's theorem, and this sum is therefore zero. On the other hand, the sum equals that over the insertion poles alone, $\sum_{i=1}^8 \text{Res}_{\mathcal{G}_i}$, because the contributions from the pinching points cancel owing to Eq. (3.11). We thus conclude that the residues at the insertion poles always sum to zero, and the set of contours encircling insertion poles alone does not constitute a complete homology basis on $\mathcal{S}_1 \cup \mathcal{S}_2$.

B. Master contours—General four-mass kinematics

Generalized discontinuity operators for the planar double box are given as eightfold contour integrals, which factor into a sevenfold contour integral localizing the integrand onto the heptacut solution surface—the joint solution of the on-shell equations for all seven propagator momenta. The last contour integral is now a contour integral on that Riemann surface. The contour cannot be chosen arbitrarily, however. It is subject to the consistency requirement that it yield a vanishing integration for any function that integrates to zero on the original contour of integration for the Feynman integral, $\mathbb{R}^D \times \mathbb{R}^D$. This ensures that two integrals which are equal, for example by virtue of nontrivial integral relations, have the same generalized cut:

$$\text{Int}_1 = \text{Int}_2 \Rightarrow \text{GenDisc}(\text{Int}_1) = \text{GenDisc}(\text{Int}_2). \quad (3.14)$$

Examples of terms which integrate to zero on $\mathbb{R}^D \times \mathbb{R}^D$ include parity-odd terms and total derivatives used in the integration-by-parts identities to reexpress a large set of formally irreducible integrals in terms of linearly independent master integrals.

We may write a general contour for a GDO as follows:

$$\sum_i \omega_i C_i, \quad (3.15)$$

where the ω_i are complex coefficients, and where the sum is taken over a linearly independent homology basis (or over an overcomplete one). For double-box integrals belonging to class (a), it turns out that consistency with IBP relations imposes no constraints on the contour and hence no constraints on the ω_i . On the other hand, the vanishing integration of (parity-odd) Levi-Civita numerator insertions—such as $\varepsilon(\ell_1, k_1, k_2, k_4)$ —results in the following constraints on the coefficients ω_i :

$$\begin{aligned} 2\omega_1 - 2\omega_2 - \omega_9 + \omega_{10} &= 0, & 2\omega_3 - 2\omega_4 - \omega_9 + \omega_{10} &= 0, \\ 2\omega_5 - 2\omega_6 - \omega_9 + \omega_{10} &= 0, & 2\omega_7 - 2\omega_8 - \omega_9 + \omega_{10} &= 0. \end{aligned} \quad (3.16)$$

In class (a), there are four linearly independent double-box integrals which we may choose to be

$$(I_1, I_2, I_3, I_4) = (P_{2,2}^{**}[1], P_{2,2}^{**}[\ell_1 \cdot k_4], P_{2,2}^{**}[\ell_2 \cdot k_1], P_{2,2}^{**}[(\ell_1 \cdot k_4)(\ell_2 \cdot k_1)]). \quad (3.17)$$

The residues at the global poles ($\mathcal{G}_1, \dots, \mathcal{G}_{10}$) of these integrals are as follows:

$$\begin{aligned} \text{Res}_{\mathcal{G}_i} P_{2,2}^{**}[1] &= \frac{\bar{\xi}'_1(\bar{\xi}'_4 - \tau \bar{\xi}'_3)}{\sqrt{\Delta}} (0, 0, 0, 0, 0, 0, 0, 0, 1, 1), \\ \text{Res}_{\mathcal{G}_i} P_{2,2}^{**}[\ell_1 \cdot k_4] &= \frac{\bar{\xi}'_1(\bar{\xi}'_4 - \tau \bar{\xi}'_3)}{\sqrt{\Delta}} (0, 0, r_4, r_4, 0, 0, -r_4, -r_4, r_2, r_2), \\ \text{Res}_{\mathcal{G}_i} P_{2,2}^{**}[\ell_2 \cdot k_1] &= \frac{\bar{\xi}'_1(\bar{\xi}'_4 - \tau \bar{\xi}'_3)}{\sqrt{\Delta}} (r_3, r_3, 0, 0, -r_3, -r_3, 0, 0, r_1, r_1), \\ \text{Res}_{\mathcal{G}_i} P_{2,2}^{**}[(\ell_1 \cdot k_4)(\ell_2 \cdot k_1)] &= \frac{\bar{\xi}'_1(\bar{\xi}'_4 - \tau \bar{\xi}'_3)}{\sqrt{\Delta}} (r_6, r_6, r_7, r_7, r_8, r_8, r_5, r_5, r_1 r_2, r_1 r_2), \end{aligned} \quad (3.18)$$

where the r_i are given by³

$$\begin{aligned} r_1 &= -\frac{1}{2} \left(2\bar{\xi}'_2 k_1^b \cdot k_2^b \frac{k_1^b \cdot k_4^b}{k_2^b \cdot k_4^b} + \bar{\xi}'_1 m_1^2 \right), & r_2 &= -\frac{1}{2} \left(2\bar{\xi}'_3 k_3^b \cdot k_4^b \frac{k_1^b \cdot k_4^b}{k_1^b \cdot k_3^b} + \bar{\xi}'_4 m_4^2 \right), & r_3 &= \frac{1 [1^b 4^b] \sqrt{\Delta}}{2 [1^b 3^b] \tau \bar{\xi}'_2 - \bar{\xi}'_1} \langle 4^b | k_1 | 3^b \rangle, \\ r_4 &= \frac{1 [1^b 4^b] \sqrt{\Delta}}{2 [2^b 4^b] \tau \bar{\xi}'_3 - \bar{\xi}'_4} \langle 1^b | k_4 | 2^b \rangle, & r_5 &= \frac{1}{4} m_1^2 \sqrt{\Delta} \frac{\langle 3^b 4^b \rangle [1^b 4^b]}{\langle 1^b 3^b \rangle [1^b 2^b]} \langle 1^b | k_4 | 2^b \rangle, & r_6 &= \frac{1}{4} m_4^2 \sqrt{\Delta} \frac{\langle 1^b 2^b \rangle [1^b 4^b]}{\langle 4^b 2^b \rangle [3^b 4^b]} \langle 4^b | k_1 | 3^b \rangle, \\ r_7 &= \frac{1}{2} k_1^b \cdot k_4^b \sqrt{\Delta} \frac{[3^b 4^b] [1^b 2^b]}{[2^b 3^b] [2^b 4^b]} \langle 1^b | k_4 | 2^b \rangle, & r_8 &= \frac{1}{2} k_1^b \cdot k_4^b \sqrt{\Delta} \frac{[1^b 2^b] [3^b 4^b]}{[3^b 2^b] [1^b 3^b]} \langle 4^b | k_1 | 3^b \rangle. \end{aligned} \quad (3.20)$$

At this point, let us choose a linearly independent homology basis for $\mathcal{S}_1 \cup \mathcal{S}_2$ consisting of the small circles $C_{3, \dots, 10}$ encircling the global poles (\mathcal{G}_i) _{$i=3, \dots, 10$} . This leaves us with eight coefficients, one for each C_j , subject to the four constraints in Eq. (3.16). Overall, we are left with four independent coefficients, the same as the number of class (a) double-box master integrals, as given in Eq. (3.17).

We can solve for these independent coefficients, finding a unique solution which yields one when applied to one of the master integrals and zero to the others. There are four such solutions, one for each master integral. We refer to the contours as *projectors* or *master contours* and to the operations of replacing the original integration contour by one of these contours and performing the contour integrals as the GDO. Each GDO uniquely extracts the coefficient of one of the master integrals in the basis decomposition (1.1) of the two-loop amplitude. Using the homology basis specified above, the master contours

$$\Gamma_j = \Omega_j \cdot \mathbf{C} = \sum_{i=3}^{10} \omega_{j,i} C_i \quad (3.21)$$

associated with the master integrals I_j in Eq. (3.17) are given by the following coefficients:

³Note that as expected $\sum_{i=1}^8 \text{Res}_{\mathcal{G}_i} I_j = 0$ for all four master integrals as

$$r_5 + r_6 + r_7 + r_8 = 0, \quad (3.19)$$

consistent with the discussion below Eq. (3.13).

$$\begin{aligned}
 I_1: \Omega_1 &= \frac{\sqrt{\Delta}}{\xi_1'(\xi_4' - \tau\xi_3')} \left(-\frac{r_2r_3r_5 + r_1r_4(r_2r_3 + r_8)}{2r_3r_4(r_5 + r_7)}, -\frac{r_2r_3r_5 + r_1r_4(r_2r_3 + r_8)}{2r_3r_4(r_5 + r_7)}, \frac{r_1}{2r_3}, \frac{r_1}{2r_3}, \frac{r_2r_3r_7 - r_1r_4(r_2r_3 + r_8)}{2r_3r_4(r_5 + r_7)}, \right. \\
 &\quad \left. \frac{r_2r_3r_7 - r_1r_4(r_2r_3 + r_8)}{2r_3r_4(r_5 + r_7)}, \frac{1}{2}, \frac{1}{2} \right), \\
 I_2: \Omega_2 &= \frac{\sqrt{\Delta}}{\xi_1'(\xi_4' - \tau\xi_3')} \frac{1}{2r_4(r_5 + r_7)} (r_5, r_5, 0, 0, -r_7, -r_7, 0, 0), \\
 I_3: \Omega_3 &= \frac{\sqrt{\Delta}}{\xi_1'(\xi_4' - \tau\xi_3')} \frac{1}{2r_3(r_5 + r_7)} (r_8, r_8, -r_5 - r_7, -r_5 - r_7, r_8, r_8, 0, 0), \\
 I_4: \Omega_4 &= \frac{\sqrt{\Delta}}{\xi_1'(\xi_4' - \tau\xi_3')} \frac{1}{2(r_5 + r_7)} (1, 1, 0, 0, 1, 1, 0, 0). \tag{3.22}
 \end{aligned}$$

(In Refs. [79,80], these coefficients were labeled P_j .) In terms of these contours, the double-box coefficients in the basis expansion (1.1) are given by the following formula:

$$\text{coefficient}_j = \oint_{\Gamma_j} dz J_{\mathcal{F}}^{(a,i)} \prod_{v=1}^6 A_{(v)}^{\text{tree}}(z), \tag{3.23}$$

where the Jacobian of Eq. (3.12), $J_{\mathcal{F}}^{(a,i)}$, is evaluated on solution \mathcal{S}_1 or \mathcal{S}_2 , according to the location of the poles encircled by Γ_j .

C. Master contours—Equal-mass case

In the special-kinematics situation where $k_1^2 = k_4^2 = m_1^2$ and $k_2^2 = k_3^2 = m_2^2$, all Lorentz scalars are invariant under $(k_1, k_2) \leftrightarrow (k_4, k_3)$, and one additional integral identity arises:

$$P_{2,2}^{**}[\ell_1 \cdot k_4] = P_{2,2}^{**}[\ell_2 \cdot k_1]. \tag{3.24}$$

We note that this identity does not arise as an IBP relation. This identity may be used to eliminate one of the integrals in Eq. (3.17), leaving us with three independent master integrals whose associated master contours we provide below. (Other special cases, such as $k_1^2 = k_3^2 = m_1^2$ and $k_2^2 = k_4^2 = m_2^2$, can be treated similarly.)

With equal-mass kinematics, all ten global poles in Eq. (3.13) remain distinct. In terms of the quantities

$$\begin{aligned}
 \rho_1 &= -\frac{m_1^2}{2}, & \rho_2 &= -\frac{(\gamma_{12} + m_2^2)k_1^b \cdot k_4^b \sqrt{\Delta}}{s_{12} \xi_1'}, \\
 \rho_3 &= \frac{m_1^2(m_2^2 + \gamma_{12})k_1^b \cdot k_4^b \sqrt{\Delta}}{2(m_1^2 + \gamma_{12})\xi_1'}, & \rho_4 &= \frac{\gamma_{12}k_1^b \cdot k_4^b \sqrt{\Delta}}{2\xi_1'}, \tag{3.25}
 \end{aligned}$$

the residues at the global poles $(\mathcal{G}_1, \dots, \mathcal{G}_{10})$ of the four integrals in Eq. (3.17) take the form

$$\begin{aligned}
 \text{Res}_{\mathcal{G}_i} P_{2,2}^{**}[1] &= \frac{\xi_1'}{\sqrt{\Delta}} \frac{s_{12}}{(\gamma_{12} + m_1^2)} (0, 0, 0, 0, 0, 0, 0, 0, 1, 1), \\
 \text{Res}_{\mathcal{G}_i} P_{2,2}^{**}[\ell_1 \cdot k_4] &= \frac{\xi_1'}{\sqrt{\Delta}} \frac{s_{12}}{(\gamma_{12} + m_1^2)} (0, 0, \rho_2, \rho_2, 0, 0, -\rho_2, -\rho_2, \rho_1, \rho_1), \\
 \text{Res}_{\mathcal{G}_i} P_{2,2}^{**}[\ell_2 \cdot k_1] &= \frac{\xi_1'}{\sqrt{\Delta}} \frac{s_{12}}{(\gamma_{12} + m_1^2)} (\rho_2, \rho_2, 0, 0, -\rho_2, -\rho_2, 0, 0, \rho_1, \rho_1), \\
 \text{Res}_{\mathcal{G}_i} P_{2,2}^{**}[(\ell_1 \cdot k_4)(\ell_2 \cdot k_1)] &= \frac{\xi_1'}{\sqrt{\Delta}} \frac{s_{12}}{(\gamma_{12} + m_1^2)} (\rho_3, \rho_3, \rho_4, \rho_4, -\rho_4, -\rho_4, -\rho_3, -\rho_3, \rho_1^2, \rho_1^2). \tag{3.26}
 \end{aligned}$$

We may use the identity (3.24) to eliminate one of the integrals in Eq. (3.17), leaving us with the master integrals

$$(I_1, I_2, I_3) = (P_{2,2}^{**}[1], P_{2,2}^{**}[\ell_1 \cdot k_4], P_{2,2}^{**}[(\ell_1 \cdot k_4)(\ell_2 \cdot k_1)]). \tag{3.27}$$

The requirement that the heptacut contour respect the identity (3.24) yields the contour constraint

$$\omega_1 + \omega_2 - \omega_3 - \omega_4 - \omega_5 - \omega_6 + \omega_7 + \omega_8 = 0. \tag{3.28}$$

In terms of the basis of homology specified in Sec. III B, the master contours Γ_j associated with the master integrals in Eq. (3.27) take the form

$$\begin{aligned}
I_1: \Omega_1 &= \frac{\sqrt{\Delta}(\gamma_{12} + m_1^2)}{2\tilde{\xi}'_1} \frac{\rho_1}{s_{12}} \frac{1}{\rho_2} \left(\frac{\rho_1\rho_2 - \rho_3 - \rho_4}{\rho_3 - \rho_4}, \frac{\rho_1\rho_2 - \rho_3 - \rho_4}{\rho_3 - \rho_4}, 1, 1, \frac{\rho_1\rho_2 - 2\rho_4}{\rho_3 - \rho_4}, \frac{\rho_1\rho_2 - 2\rho_4}{\rho_3 - \rho_4}, \frac{\rho_2}{\rho_1}, \frac{\rho_2}{\rho_1} \right), \\
I_2: \Omega_2 &= \frac{\sqrt{\Delta}(\gamma_{12} + m_1^2)}{2\tilde{\xi}'_1} \frac{1}{s_{12}} \frac{1}{\rho_2} \left(\frac{\rho_3 + \rho_4}{\rho_3 - \rho_4}, \frac{\rho_3 + \rho_4}{\rho_3 - \rho_4}, -1, -1, \frac{2\rho_4}{\rho_3 - \rho_4}, \frac{2\rho_4}{\rho_3 - \rho_4}, 0, 0 \right), \\
I_3: \Omega_3 &= -\frac{\sqrt{\Delta}(\gamma_{12} + m_1^2)}{2\tilde{\xi}'_1} \frac{1}{s_{12}} \frac{1}{(\rho_3 - \rho_4)} (1, 1, 0, 0, 1, 1, 0, 0). \tag{3.29}
\end{aligned}$$

One is not obliged to make use of the integral identity (3.24) and enforce the ensuing contour constraint (3.28); one could equally well expand the equal-mass amplitude in terms of the slightly overcomplete basis in Eq. (3.17), with the associated master contours given in Eq. (3.22). Indeed, since the energies of heavy particles follow a Breit-Wigner distribution, an amplitude involving four massive vector bosons (e.g., $WZ \rightarrow WZ$) will typically be required only for unequal masses; only when taking the on-shell approximation would the equal-mass case arise.

IV. ALGEBRAIC VARIETIES ARISING FROM FEYNMAN GRAPHS

In this section we discuss the heptacut of the planar double-box integral, putting some of the observations in Sec. III into the broader context of algebraic geometry.

On-shell constraints are polynomial equations. Accordingly, their simultaneous solution defines an algebraic variety. Reference [82] observed that the variety corresponding to setting all seven propagator momenta of the planar double box on shell is a pinched torus, with the number of pinches equal to twice the number of double-box rungs that end on at least one three-point vertex. As mentioned in the previous section and in Ref. [80], we denote integrals having one, two, or three such rungs as forming classes (a), (b), and (c). The respective pinched tori—*nodal elliptic curves*, in the language of mathematicians—are illustrated in Figs. 3(a), 3(b), and 3(c).

The components of the pinched tori are Riemann spheres. These spheres are associated with distinct solutions to the joint on-shell constraints (3.4) and are characterized by the distribution of chiralities (● or ○) at the vertices of the double-box graph. The fact that the number of pinches is always even is a reflection of the fact that the on-shell solutions always come in parity-conjugate pairs. At a pinching point, there is exactly one double-box rung whose momentum becomes collinear with the massless external momenta connected to the rung. For the original uncut double-box integral, such regions of the loop-momentum integration typically produce infrared divergences, and the pinches can therefore roughly be thought of as remnants of the original IR divergences. In addition, the pinched tori contain a number of insertion points [for example, in Fig. 3(a), the points $\mathcal{G}_1, \dots, \mathcal{G}_8$] where one of the loop momenta becomes infinite. Because the order of the pole is related to the ultraviolet power counting of underlying integrals in the theory (taking into account fermion-boson cancellations), these insertion points can be associated, roughly speaking, with UV divergences.

The pattern of global poles in classes (a)–(c) can be understood as follows. Starting from Fig. 3(a), we can imagine taking massless limits of external momenta, at each step having exactly one additional double-box rung end on a three-point vertex. Geometrically, each step adds a pair of pinches (nodal points)—the first step producing Fig. 3(b), and the second producing Fig. 3(c). Each pinch preserves the global poles already present and adds a global pole at the location of the pinching point. Nonetheless, pinching leaves the number of *independent* global poles constant: while it creates a new global pole, it also creates a new Riemann sphere and hence adds a global residue constraint which allows one global pole to be eliminated. There are eight independent global poles in class (a), and the number remains eight in classes (b) and (c).

To be more specific, class (b) contains 12 global poles, as illustrated in Fig. 3(b). The poles $\mathcal{G}_1, \dots, \mathcal{G}_{10}$ are obtained by taking the limit $\tilde{\xi}'_3 \rightarrow 0$ (corresponding to either $m_3 \rightarrow 0$ or $m_4 \rightarrow 0$) of the class (a) poles in Eq. (3.13).⁴

⁴For convenience, we note that the labeling of global poles here is related to that of Ref. [80] as follows:

$$\begin{aligned}
(\mathcal{G}_1^{(b)}, \mathcal{G}_2^{(b)}, \mathcal{G}_3^{(b)}, \mathcal{G}_4^{(b)}, \mathcal{G}_5^{(b)}, \mathcal{G}_6^{(b)}, \mathcal{G}_7^{(b)}, \mathcal{G}_8^{(b)})^{[80]} &= (\mathcal{G}_9^{(b)}, \mathcal{G}_{10}^{(b)}, \mathcal{G}_{11}^{(b)}, \mathcal{G}_{12}^{(b)}, \mathcal{G}_3^{(b)}, \mathcal{G}_4^{(b)}, \mathcal{G}_5^{(b)}, \mathcal{G}_6^{(b)}), \\
(\mathcal{G}_1^{(c)}, \mathcal{G}_2^{(c)}, \mathcal{G}_3^{(c)}, \mathcal{G}_4^{(c)}, \mathcal{G}_5^{(c)}, \mathcal{G}_6^{(c)}, \mathcal{G}_7^{(c)}, \mathcal{G}_8^{(c)})^{[80]} &= (\mathcal{G}_9^{(c)}, \mathcal{G}_{10}^{(c)}, \mathcal{G}_{11}^{(c)}, \mathcal{G}_{12}^{(c)}, \mathcal{G}_{14}^{(c)}, \mathcal{G}_{13}^{(c)}, \mathcal{G}_5^{(c)}, \mathcal{G}_6^{(c)}),
\end{aligned}$$

where the labeling on the left-hand sides corresponds to that of Eqs. (4.16) and (4.27) of Ref. [80]. The labeling on the right-hand sides is that of the present paper, with the superscript (b) denoting that one should take the $\tilde{\xi}'_3 \rightarrow 0$ limit of the poles listed in Eq. (3.13) to obtain the class (b) poles, and the superscript (c) indicating that one should further take the limit $\tilde{\xi}'_2 \rightarrow 0$ to find the class (c) poles.

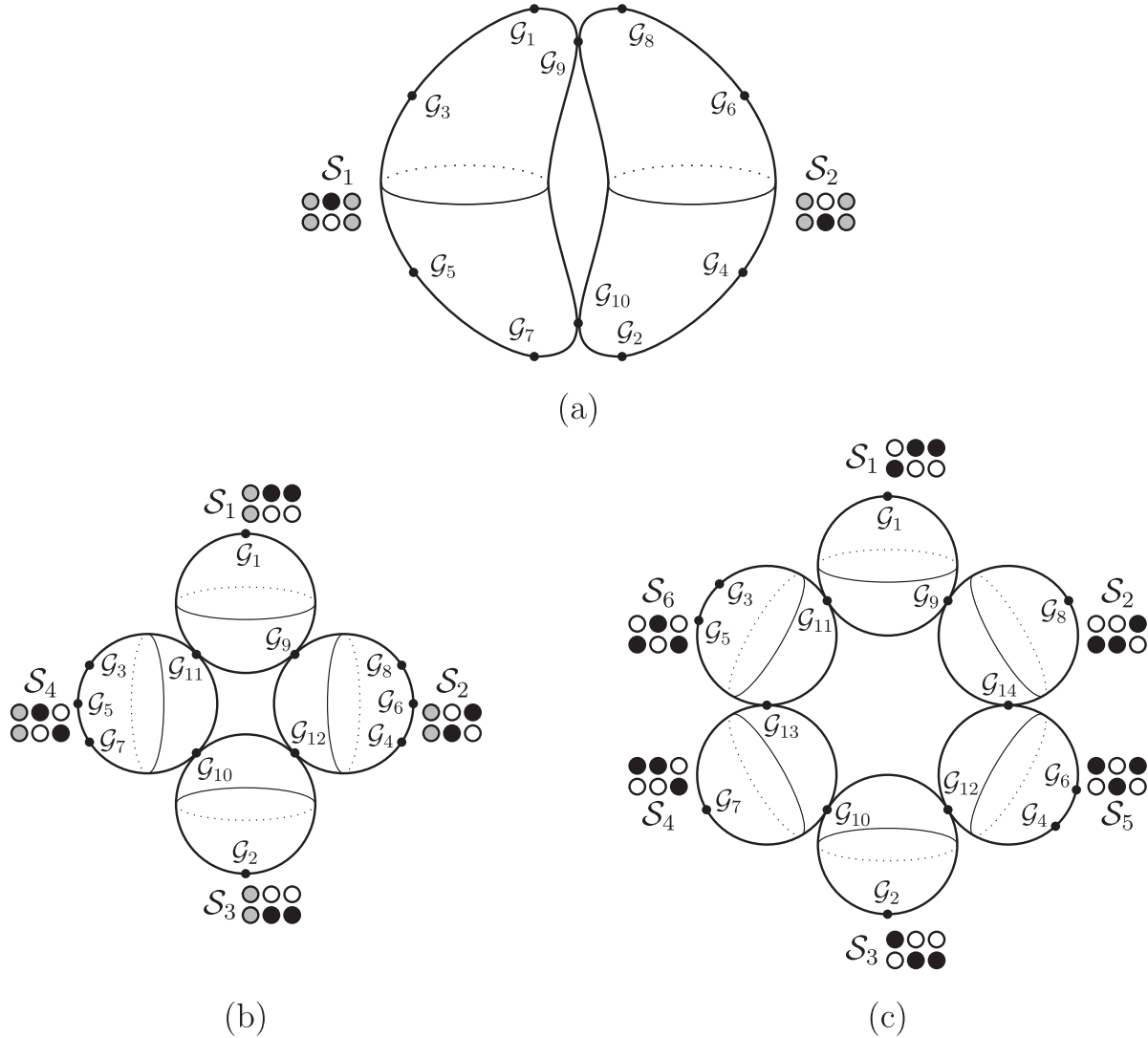


FIG. 3. Representations of the solution space for the class (a), (b), and (c) heptacut equations, showing the independent solutions \mathcal{S}_i , and the locations of the global poles \mathcal{G}_j .

As evaluating the limit of \mathcal{G}_9 and \mathcal{G}_{10} is slightly subtle, we quote the result here:

$$\begin{aligned} \mathcal{G}_9: \lim_{\bar{\xi}'_3 \rightarrow 0} \left(z_+, \frac{\bar{\xi}'_2}{z_+}, -\frac{(z_+ \bar{\xi}'_1 + \tau \bar{\xi}'_2) \bar{\xi}'_3}{(z_+ \bar{\xi}'_1 + \bar{\xi}'_2) \bar{\xi}'_4}, -\frac{(z_+ \bar{\xi}'_1 + \bar{\xi}'_2) \bar{\xi}'_4}{z_+ \bar{\xi}'_1 + \tau \bar{\xi}'_2} \right) &= \left(-\frac{\bar{\xi}'_2}{\bar{\xi}'_1}, -\bar{\xi}'_1, \frac{\bar{\xi}'_2 - \bar{\xi}'_1}{\bar{\xi}'_1 - \tau \bar{\xi}'_2}, 0 \right), \\ \mathcal{G}_{10}: \lim_{\bar{\xi}'_3 \rightarrow 0} \left(z_-, \frac{\bar{\xi}'_2}{z_-}, -\frac{1 + z_-}{1 + \tau z_-}, -\frac{(1 + \tau z_-) \bar{\xi}'_3}{1 + z_-} \right) &= \left(-1, -\bar{\xi}'_2, 0, -\frac{(\bar{\xi}'_1 - \bar{\xi}'_2) \bar{\xi}'_4}{\bar{\xi}'_1 - \tau \bar{\xi}'_2} \right). \end{aligned} \quad (4.1)$$

In addition, class (b) contains the following two global poles:

$$\mathcal{G}_{11}: \left(-\frac{\bar{\xi}'_2}{\bar{\xi}'_1}, -\bar{\xi}'_1, 0, 0 \right), \quad \mathcal{G}_{12}: (-1, -\bar{\xi}'_2, 0, 0), \quad (4.2)$$

which are exactly the two nodal points created during the pinches $\mathcal{S}_1 \rightarrow \mathcal{S}_1 \cup \mathcal{S}_4$ and $\mathcal{S}_2 \rightarrow \mathcal{S}_2 \cup \mathcal{S}_3$ [compare Figs. 3(a) and 3(b)]. Similarly, class (c) contains 14 global poles, as illustrated in Fig. 3(c). The poles $\mathcal{G}_1, \dots, \mathcal{G}_{12}$ are

obtained by taking the limit $\bar{\xi}'_2 \rightarrow 0$ (corresponding to either $m_1 \rightarrow 0$ or $m_2 \rightarrow 0$) of the class (b) global poles. In addition, class (c) contains the following two global poles:

$$\mathcal{G}_{13}: (0, 0, 0, -\bar{\xi}'_4), \quad \mathcal{G}_{14}: (0, 0, -1, 0), \quad (4.3)$$

which are precisely the two nodal points created during the pinches $\mathcal{S}_4 \rightarrow \mathcal{S}_4 \cup \mathcal{S}_6$ and $\mathcal{S}_2 \rightarrow \mathcal{S}_2 \cup \mathcal{S}_5$ [compare Figs. 3(b) and 3(c)].

As explained in Sec. III, contours for GDOs must annihilate any function that integrates to zero on $\mathbb{R}^D \times \mathbb{R}^D$. In terms of the coefficients ω_i of the basis contours C_j , this requirement yields the following constraints from numerator insertions of Levi-Civita tensors (which are parity odd):

$$\begin{aligned} 2\omega_1 - 2\omega_2 - \omega_9 + \omega_{10} + \omega_{11} - \omega_{12} + \omega_{13} - \omega_{14} &= 0, \\ 2\omega_3 - 2\omega_4 - \omega_9 + \omega_{10} - \omega_{11} + \omega_{12} + \omega_{13} - \omega_{14} &= 0, \\ 2\omega_5 - 2\omega_6 - \omega_9 + \omega_{10} - \omega_{11} + \omega_{12} + \omega_{13} - \omega_{14} &= 0, \\ 2\omega_7 - 2\omega_8 - \omega_9 + \omega_{10} - \omega_{11} + \omega_{12} - \omega_{13} + \omega_{14} &= 0, \end{aligned} \quad (4.4)$$

where $\omega_{11,12,13,14} \rightarrow 0$ in class (a) and $\omega_{13,14} \rightarrow 0$ in class (b). If we choose a homology basis consisting of parity-conjugate pairs of poles, these constraints are expressed by the simple geometric statement that a valid contour must be invariant under a rotation through π radians of Figs. 3(a), 3(b), and 3(c), respectively.

Consistency with IBP identities imposes less transparent constraints on maximal-cut contours. In class (b), there is a single IBP constraint which takes the form

$$\begin{aligned} 2\omega_1 + 2\omega_2 - \omega_3 - \omega_4 - \omega_7 - \omega_8 \\ - \omega_9 - \omega_{10} + \omega_{11} + \omega_{12} &= 0, \end{aligned} \quad (4.5)$$

whereas in class (c) there are two IBP constraints which take the form

$$\begin{aligned} 2\omega_1 + 2\omega_2 - \omega_3 - \omega_4 - \omega_7 - \omega_8 \\ - \omega_9 - \omega_{10} + \omega_{11} + \omega_{12} &= 0, \end{aligned} \quad (4.6)$$

$$\begin{aligned} \omega_3 + \omega_4 + 2\omega_5 + 2\omega_6 - 3\omega_7 - 3\omega_8 - \omega_9 - \omega_{10} \\ - \omega_{11} - \omega_{12} + 2\omega_{13} + 2\omega_{14} &= 0. \end{aligned} \quad (4.7)$$

The first class (c) constraint (4.6) is identical to the class (b) one in Eq. (4.5). This suggests that these constraints arise during the pinchings that carry the doubly pinched torus depicted in Fig. 3(a) into the quadruply pinched torus of Fig. 3(b) and thence into the sextuply pinched torus of Fig. 3(c). The transition from Fig. 3(a) into Fig. 3(b) involves two (parity-conjugate) pinches which one might at first expect to produce two constraints. However, as a valid contour must be parity symmetric (4.4), we should really expect *one* independent constraint to arise from a double pinching. This constraint is accompanied by a second constraint arising from the double pinching that turns Fig. 3(b) into Fig. 3(c). This pattern offers hope that it may be possible to derive the IBP constraints (4.5)–(4.7) directly from the underlying algebraic geometry.

Expressing the IBP constraints in an overcomplete basis of homology makes it clear that they cannot be determined from algebraic *topology* alone. For example, on the sphere \mathcal{S}_4 in Fig. 3(b), the poles $\mathcal{G}_3, \mathcal{G}_5, \mathcal{G}_7$ may be freely relabeled among each other without changing the topology. In contrast, Eq. (4.5) does not have this relabeling symmetry.

A. Discrete symmetries of IBP constraints

We observe that the class (b) IBP constraint (4.5) is symmetric under reflection of Fig. 3(b) in the vertical axis passing through the poles \mathcal{G}_1 and \mathcal{G}_2 . More explicitly, Eq. (4.5) is symmetric under the interchanges⁵

$$\begin{aligned} \omega_1 &\leftrightarrow \omega_1, & \omega_5 &\leftrightarrow \omega_6, \\ \omega_2 &\leftrightarrow \omega_2, & \omega_9 &\leftrightarrow -\omega_{11}, \\ \omega_3 &\leftrightarrow \omega_8, & \omega_{10} &\leftrightarrow -\omega_{12}, \\ \omega_4 &\leftrightarrow \omega_7, \end{aligned} \quad (4.8)$$

The pattern of relative minuses in Eq. (4.8) owes to the fact that, in our orientation conventions, the reflection flips the orientation of the pinching or “IR” cycles but preserves that of the insertion or “UV” cycles.

Conversely, assuming the symmetry (4.8), one might ask to what extent it determines the IBP constraint. The most general IBP constraint invariant under Eq. (4.8) takes the form

$$\begin{aligned} a_1\omega_1 + a_2\omega_2 + a_3(\omega_3 + \omega_8) + a_4(\omega_4 + \omega_7) + a_5(\omega_5 + \omega_6) \\ + a_6(\omega_9 - \omega_{11}) + a_7(\omega_{10} - \omega_{12}) &= 0. \end{aligned} \quad (4.9)$$

For convenience, let us now choose a basis of homology, for example $\omega_{1,2,5,6} = 0$. In this basis, the IBP constraint (4.9) takes the form

$$\begin{aligned} r_1^{(b)}(\omega_3 + \omega_4 + \omega_7 + \omega_8) \\ + r_2^{(b)}(\omega_9 + \omega_{10} - \omega_{11} - \omega_{12}) &= 0, \end{aligned} \quad (4.10)$$

where we furthermore imposed the Levi-Civita constraints (4.4). Remarkably, the only thing left unexplained by the flip symmetry (4.8) is the fact that $r_1^{(b)} = r_2^{(b)} \neq 0$.

Out of the two IBP constraints in class (c), we observe that Eq. (4.6) is inherited directly from Eq. (4.5) whereas the difference between Eqs. (4.6) and (4.7) is symmetric under reflection of Fig. 3(c) in a line passing through the centers of the spheres \mathcal{S}_5 and \mathcal{S}_6 . More explicitly, the difference is symmetric under the interchanges

⁵This symmetry does not have an obvious physical meaning: it corresponds to flipping the right loop of the double-box graph through a vertical axis.

$$\begin{aligned}
 \omega_1 &\leftrightarrow \omega_7, & \omega_9 &\leftrightarrow -\omega_{10}, \\
 \omega_2 &\leftrightarrow \omega_8, & \omega_{11} &\leftrightarrow -\omega_{13}, \\
 \omega_3 &\leftrightarrow \omega_5, & \omega_{12} &\leftrightarrow -\omega_{14}, \\
 \omega_4 &\leftrightarrow \omega_6, & &
 \end{aligned}
 \tag{4.11}$$

This symmetry will be broken by any choice of homology basis, highlighting the virtue of expressing the IBP constraints (4.6) and (4.7) in an overcomplete basis.

In analogy with the above, we can write down the most general constraint invariant under Eq. (4.11), choose a basis of homology such as $\omega_{1,2,5,6,7,8} = 0$ and impose the Levi-Civita constraints (4.4). We are then left with the constraint

$$r_1^{(c)}(\omega_3 + \omega_4) + r_2^{(c)}(\omega_{11} + \omega_{12} - \omega_{13} - \omega_{14}) = 0. \tag{4.12}$$

Only the requirement that $r_1^{(c)} = -r_2^{(c)} \neq 0$ is left unexplained by the flip symmetry (4.11).

V. CONCLUSIONS

In this paper we have extended the maximal-unitarity formalism at two loops to double-box integrals with four massive external legs. We have constructed generalized discontinuity operators which isolate each of the four master integrals, annihilating all others. Applying one of these GDOs to the amplitude yields a formula for the corresponding coefficient in Eq. (1.1), as a contour integral over products of tree-level amplitudes.

We can choose to think of each GDO as operating in two steps. In the first step, we perform seven of the eight contour integrals, thereby putting on shell all internal lines of the double-box integral. This restricts the integrand to a Riemann surface, which has the form of a multiply pinched torus. Each component is a Riemann sphere, with the number of spheres equal to twice the number of double-box rungs that end on a three-point vertex. This step is identical for all four GDOs.

In the second step, we perform the remaining contour integral over a contour on the Riemann surface. This fully localizes the integrand onto a combination of global poles. The integration contours are different for each GDO. They are subject to consistency constraints. These constraints fall into two classes for general double-box integrals: (a) parity symmetry, amounting to invariance of the contours under rotations through π radians of the pinched tori; and (b) consistency with IBP relations. Writing out the latter constraints in an overcomplete basis of homology exposes additional flip symmetries. These symmetries alone would allow us to determine the constraints up to a small number of constants. The IBP relations determine these constants.

For the four-mass double box [class (a)], the underlying Riemann surface consists of two spheres, and there is no contour constraint from IBP relations. For the three-mass and short-side two-mass double boxes [class (b)],

considered previously in Ref. [80], the Riemann surface consists of four linked spheres. It can be viewed as derived from the two-sphere Riemann surface via a double pinching. One IBP constraint arises here. This constraint is inherited by the last case, a six-sphere surface corresponding to massless, one-mass, diagonal and long-side two-mass double boxes [class (c)], considered previously in Refs. [79,80]. The six spheres again can be viewed as derived from the four-sphere surface via a double pinching, and an additional IBP constraint emerges as well. Thus, the IBP contour constraints appear to arise during the chiral branchings of the on-shell solutions, suggesting a strong connection to the underlying algebraic geometry.

This sequence of IBP constraints suggests a more natural choice of master integrals than that of Eq. (3.17). Namely, one can construct a set of four integrals with the property that in class (a) all integrals are linearly independent, whereas in classes (b) and (c), respectively, one and two elements become zero (up to terms with vanishing heptacuts), by virtue of integration-by-parts relations. (We refer to Appendix B for an explicit construction of such a set of integrals.)

A complete calculation of four-point amplitudes will also require the $\mathcal{O}(\epsilon)$ terms in integral coefficients and also GDOs for integrals with fewer than seven propagators. For processes with additional external legs, higher-point integrals will be needed as well. The simplest extension would probably be to ‘‘turtle-box’’ integrals ($P_{2,2}^*$ in the notation of Ref. [83]), as their properties are related to those of the double-box integrals considered here and in Refs. [79,80].

The generalized discontinuity operators whose contours are given by Eqs. (3.15) and (3.22), along with similar results from Ref. [80], can be applied directly to computations of two-loop amplitudes in both numerical and analytic forms. Their construction also hints at deeper connections to the algebraic geometry of the corresponding Feynman integrals.

ACKNOWLEDGMENTS

K. J. L. thanks CERN and the Institute for Advanced Study in Princeton, where part of this work was carried out, for their hospitality. We also thank Spencer Bloch, Simon Caron-Huot, Benjamin Matschke and Masahiko Taniguchi for useful discussions. This work was supported in part by the Research Executive Agency (REA) of the European Union under Grant Agreement No. PITN-GA-2010-264564 (LHCPhenoNet). This work is supported by the European Research Council under Advanced Investigator Grant No. ERC-AdG-228301.

APPENDIX A: EXPLICIT LOOP MOMENTA

In this Appendix, we present explicit forms for the loop momenta in the two solutions $\mathcal{S}_{1,2}$ of the four-mass planar double-box heptacut equations. Solution \mathcal{S}_2 is given explicitly by

$$\begin{aligned}\ell_1^\mu &= \bar{\xi}'_1 \left(k_1^{b,\mu} + \frac{z \langle 1^b 4^b \rangle}{2 \langle 2^b 4^b \rangle} \langle 2^b | \gamma^\mu | 1^b \rangle \right) + \bar{\xi}'_2 \frac{k_1^b \cdot k_4^b}{k_2^b \cdot k_4^b} \left(k_2^{b,\mu} + \frac{1 \langle 2^b 4^b \rangle}{2z \langle 1^b 4^b \rangle} \langle 1^b | \gamma^\mu | 2^b \rangle \right), \\ \ell_2^\mu &= \bar{\xi}'_4 \left(k_4^{b,\mu} + \frac{w \langle 1^b 4^b \rangle}{2 \langle 1^b 3^b \rangle} \langle 3^b | \gamma^\mu | 4^b \rangle \right) + \bar{\xi}'_3 \frac{k_1^b \cdot k_4^b}{k_1^b \cdot k_3^b} \left(k_3^{b,\mu} + \frac{1 \langle 1^b 3^b \rangle}{2w \langle 1^b 4^b \rangle} \langle 4^b | \gamma^\mu | 3^b \rangle \right),\end{aligned}\quad (\text{A1})$$

where

$$w = -\frac{z+1}{z\tau+1}.\quad (\text{A2})$$

Solution \mathcal{S}_2 has poles corresponding to infinite momenta located at $z = \{0, \infty, -1, -1/\tau\}$ or, alternatively, at $w = \{-1, -1/\tau, 0, \infty\}$. For the first two ℓ_1^μ is infinite, and ℓ_2^μ takes the finite values

$$\begin{aligned}\mathcal{G}_8: \ell_2^\mu(z=0) &= \bar{\xi}'_4 \left(k_4^{b,\mu} - \frac{1 \langle 1^b 4^b \rangle}{2 \langle 1^b 3^b \rangle} \langle 3^b | \gamma^\mu | 4^b \rangle \right) + \bar{\xi}'_3 \frac{k_1^b \cdot k_4^b}{k_1^b \cdot k_3^b} \left(k_3^{b,\mu} - \frac{1 \langle 1^b 3^b \rangle}{2 \langle 1^b 4^b \rangle} \langle 4^b | \gamma^\mu | 3^b \rangle \right), \\ \mathcal{G}_4: \ell_2^\mu(z=\infty) &= \bar{\xi}'_4 \left(k_4^{b,\mu} - \frac{1 \langle 2^b 4^b \rangle}{2 \langle 2^b 3^b \rangle} \langle 3^b | \gamma^\mu | 4^b \rangle \right) + \bar{\xi}'_3 \frac{k_1^b \cdot k_4^b}{k_1^b \cdot k_3^b} \left(k_3^{b,\mu} - \frac{1 \langle 2^b 3^b \rangle}{2 \langle 2^b 4^b \rangle} \langle 4^b | \gamma^\mu | 3^b \rangle \right).\end{aligned}\quad (\text{A3})$$

These two values are related by a swap of legs $1 \leftrightarrow 2$. For the latter two poles ℓ_2^μ is infinite, and ℓ_1^μ takes the finite values

$$\begin{aligned}\mathcal{G}_2: \ell_1^\mu(z=-1) &= \bar{\xi}'_1 \left(k_1^{b,\mu} - \frac{1 \langle 1^b 4^b \rangle}{2 \langle 2^b 4^b \rangle} \langle 2^b | \gamma^\mu | 1^b \rangle \right) + \bar{\xi}'_2 \frac{k_1^b \cdot k_4^b}{k_2^b \cdot k_4^b} \left(k_2^{b,\mu} - \frac{1 \langle 2^b 4^b \rangle}{2 \langle 1^b 4^b \rangle} \langle 1^b | \gamma^\mu | 2^b \rangle \right), \\ \mathcal{G}_6: \ell_1^\mu\left(z=-\frac{1}{\tau}\right) &= \bar{\xi}'_1 \left(k_1^{b,\mu} - \frac{1 \langle 1^b 3^b \rangle}{2 \langle 2^b 3^b \rangle} \langle 2^b | \gamma^\mu | 1^b \rangle \right) + \bar{\xi}'_2 \frac{k_1^b \cdot k_4^b}{k_2^b \cdot k_4^b} \left(k_2^{b,\mu} - \frac{1 \langle 2^b 3^b \rangle}{2 \langle 1^b 3^b \rangle} \langle 1^b | \gamma^\mu | 2^b \rangle \right),\end{aligned}\quad (\text{A4})$$

which are related by the swap of legs $3 \leftrightarrow 4$. (Moreover, as should be clear from the left-right symmetry of the double box, there is a map $\{1, 2, \ell_1, z\} \leftrightarrow \{4, 3, \ell_2, w\}$ that relates the above two pairs of poles.)

Solution \mathcal{S}_1 can be obtained from \mathcal{S}_2 by spinor conjugation $\langle ab \rangle \leftrightarrow [ba]$, along with the reparametrization $z \rightarrow z/\bar{\xi}'_1$. The values of the momenta at poles $z = \{0, \infty, -\bar{\xi}'_1, -\bar{\xi}'_1/\tau\}$ are given by

$$\begin{aligned}\mathcal{G}_7: \ell_{i,\mathcal{S}_1}^\mu(0) &= (\ell_{i,\mathcal{S}_2}^\mu(0))^\dagger, & \mathcal{G}_3: \ell_{i,\mathcal{S}_1}^\mu(\infty) &= (\ell_{i,\mathcal{S}_2}^\mu(\infty))^\dagger, \\ \mathcal{G}_1: \ell_{i,\mathcal{S}_1}^\mu(-\bar{\xi}'_1) &= (\ell_{i,\mathcal{S}_2}^\mu(-1))^\dagger, & \mathcal{G}_5: \ell_{i,\mathcal{S}_1}^\mu(-\bar{\xi}'_1/\tau) &= (\ell_{i,\mathcal{S}_2}^\mu(-1/\tau))^\dagger,\end{aligned}\quad (\text{A5})$$

where \dagger denotes spinor conjugation.

At the Jacobian poles $z = z_\pm$ for \mathcal{S}_2 , and $z = \bar{\xi}'_1 z_\pm$ for \mathcal{S}_1 , the momenta are finite and satisfy the relations

$$\begin{aligned}\ell_{1,\mathcal{S}_1}^\mu(\bar{\xi}'_1 z_\pm) &= -\ell_{2,\mathcal{S}_1}^\mu(\bar{\xi}'_1 z_\pm), & \ell_{1,\mathcal{S}_2}^\mu(z_\pm) &= -\ell_{2,\mathcal{S}_2}^\mu(z_\pm), & \ell_{i,\mathcal{S}_1}^\mu(\bar{\xi}'_1 z_\pm) &= \ell_{i,\mathcal{S}_2}^\mu(z_\mp), \\ \ell_{i,\mathcal{S}_2}^\mu(z_+) &= (\ell_{i,\mathcal{S}_2}^\mu(z_-))^\dagger, & \ell_{i,\mathcal{S}_1}^\mu(\bar{\xi}'_1 z_+) &= (\ell_{i,\mathcal{S}_1}^\mu(\bar{\xi}'_1 z_-))^\dagger.\end{aligned}\quad (\text{A6})$$

The first two relations follow because the Jacobian pole corresponds to the middle rung in the double box becoming soft, $\ell_1 + \ell_2 = 0$. The third relation is a consequence of the fact that the Jacobian pole is located on the intersection of the two spheres, $\mathcal{S}_1 \cap \mathcal{S}_2$. The fourth and fifth identities arise because the two Jacobian poles are complex conjugates. Because $\ell_1 + \ell_2 = 0$, the two distinct kinematic solutions are identical to the two quadruple-cut solutions for a one-loop four-mass box [16].

APPENDIX B: IBP-INSPIRED CHOICE FOR THE INTEGRAL BASIS

The sequence of IBP constraints (4.5)–(4.7) in classes (b) and (c) suggests natural choices of master integrals. We work out the details of such a basis here. We note that one can construct a set of four integrals with the property that in class (a) all integrals are linearly independent, whereas in classes (b) and (c), respectively, one and two basis elements drop out, because they vanish identically or become reducible via IBPs to simpler topologies.

To construct such a set of integrals, we start from the observation that in class (b) there is a unique IBP constraint, corresponding to a unique double-box numerator insertion which yields zero after integration. In the labeling of Fig. 1, case (b) corresponds to the vanishing of the product $m_3 m_4$, but there is an analogous case (b') where $m_1 m_2 = 0$. The unique residues of the IBP constraints in these two kinematic cases of the double-box integral are given by

$$\mathcal{R}_{\text{IBP}}^{(b)} = (2, 2, -1, -1, 0, 0, -1, -1, -1, -1) \quad \text{when} \\ m_3 m_4 = 0, \quad (\text{B1})$$

$$\mathcal{R}_{\text{IBP}}^{(b')} = (-1, -1, 0, 0, -1, -1, 2, 2, 1, 1) \quad \text{when} \\ m_1 m_2 = 0, \quad (\text{B2})$$

where the residues correspond to the global poles $(\mathcal{G}_i)_{i=1,\dots,10}$. Here, the list of residues in Eq. (B1) was read off from the left-hand side of the IBP constraint (4.5). The class (b') IBP constraint, for the case $m_1 m_2 = 0$, can be obtained from the $m_3 m_4 = 0$ case by relabeling the global poles and their residues according to the left-right flip of Fig. 3(a) through a vertical axis intersecting the poles \mathcal{G}_9 and \mathcal{G}_{10} . (One must take into account the flip in orientation of the cycles around the nodal points $\mathcal{G}_{9,10}$, which causes their residues to change sign.) Note that the second constraint in class (c), Eq. (4.7), precisely corresponds to the linear combination $-\mathcal{R}_{\text{IBP}}^{(b)} - 2\mathcal{R}_{\text{IBP}}^{(b')}$.

We can now construct a pair of new integrals I'_3 and I'_4 whose residues are proportional, respectively, to the two IBP residues (B1) and (B2). The *Ansätze* for the new integrals are

$$I'_3 = \sum_{j=1}^4 a_j I_j \quad \text{and} \quad I'_4 = \sum_{j=1}^4 b_j I_j, \quad (\text{B3})$$

with I_j denoting the integrals in Eq. (3.17). We determine the coefficients a_j, b_j by requiring that the residues are proportional:

$$\text{Res}_{\mathcal{G}_i} I'_3 = \sum_{j=1}^4 a_j \text{Res}_{\mathcal{G}_i} I_j \\ \propto (2, 2, -1, -1, 0, 0, -1, -1, -1, -1), \\ \text{Res}_{\mathcal{G}_i} I'_4 = \sum_{j=1}^4 b_j \text{Res}_{\mathcal{G}_i} I_j \\ \propto (-1, -1, 0, 0, -1, -1, 2, 2, 1, 1), \quad (\text{B4})$$

where the residues $\text{Res}_{\mathcal{G}_i} I_j$ are given in Eqs. (3.18) and (3.20).

Solving for a_j, b_j , one finds the following basis of integrals with the desired properties:

$$I'_1 = I_1, \\ I'_2 = I_2, \\ I'_3 = \left(\frac{r_2(r_7 - r_5)}{r_4} - \frac{2r_1 r_8}{r_3} - 2r_1 r_2 + r_5 + r_7 \right) I_1 \\ + \frac{r_5 - r_7}{r_4} I_2 + \frac{2r_8}{r_3} I_3 + 2I_4, \\ I'_4 = \left(\frac{r_1(r_8 - r_6)}{r_3} - \frac{2r_2 r_7}{r_4} + 2r_1 r_2 + r_6 + r_8 \right) I_1 \\ + \frac{2r_7}{r_4} I_2 + \frac{r_6 - r_8}{r_3} I_3 - 2I_4, \quad (\text{B5})$$

where the global residues r_i are defined in Eq. (3.20). These integrals are linearly independent in class (a), whereas in class (b), the heptacut of I'_3 vanishes for $m_3 m_4 = 0$, and the heptacut of I'_4 vanishes for $m_1 m_2 = 0$. In class (c), both I'_3 and I'_4 have vanishing heptacuts because in this class $m_1 m_2$ and $m_3 m_4$ vanish simultaneously. This is consistent with the class (c) IBP constraints in Eqs. (4.6) and (4.7) being linear combinations of the constraints corresponding to the residues in Eqs. (B1) and (B2).

-
- [1] G. Aad *et al.* (ATLAS Collaboration), *Phys. Lett. B* **716**, 1 (2012).
 [2] S. Chatrchyan *et al.* (CMS Collaboration), *Phys. Lett. B* **716**, 30 (2012).
 [3] R. K. Ellis, K. Melnikov, and G. Zanderighi, *J. High Energy Phys.* **04** (2009) 077; *Phys. Rev. D* **80**, 094002 (2009); K. Melnikov and G. Zanderighi, *Phys. Rev. D* **81**, 074025 (2010).
 [4] C. F. Berger, Z. Bern, L. J. Dixon, F. Febres Cordero, D. Forde, T. Gleisberg, H. Ita, D. A. Kosower, and D. Maître,

- Phys. Rev. Lett.* **102**, 222001 (2009); *Phys. Rev. D* **80**, 074036 (2009).
 [5] C. F. Berger, Z. Bern, L. J. Dixon, F. Febres Cordero, D. Forde, T. Gleisberg, H. Ita, D. A. Kosower, and D. Maître, *Phys. Rev. D* **82**, 074002 (2010).
 [6] C. F. Berger, Z. Bern, L. J. Dixon, F. Febres Cordero, D. Forde, T. Gleisberg, H. Ita, D. A. Kosower, and D. Maître, *Phys. Rev. Lett.* **106**, 092001 (2011).
 [7] H. Ita, Z. Bern, L. J. Dixon, F. Febres Cordero, D. A. Kosower, and D. Maître, *Phys. Rev. D* **85**, 031501 (2012).

- [8] S. Badger, B. Biedermann, P. Uwer, and V. Yundin, *Phys. Lett. B* **718**, 965 (2013).
- [9] Z. Bern, L. J. Dixon, F. Febres Cordero, S. Hoeche, H. Ita, D. A. Kosower, D. Maître, and K. J. Ozeren, *Phys. Rev. D* **88**, 014025 (2013).
- [10] A. Gehrmann-De Ridder, T. Gehrmann, E. W. N. Glover, and G. Heinrich, *J. High Energy Phys.* **11** (2007) 058; S. Weinzierl, *Phys. Rev. Lett.* **101**, 162001 (2008).
- [11] G. Dissertori, A. Gehrmann-De Ridder, T. Gehrmann, E. W. N. Glover, G. Heinrich, G. Luisoni, and H. Stenzel, *J. High Energy Phys.* **08** (2009) 036; G. Dissertori, A. Gehrmann-De Ridder, T. Gehrmann, E. W. N. Glover, G. Heinrich, and H. Stenzel, *Phys. Rev. Lett.* **104**, 072002 (2010).
- [12] Z. Bern, L. J. Dixon, D. C. Dunbar, and D. A. Kosower, *Nucl. Phys.* **B425**, 217 (1994); **B435**, 59 (1995); Z. Bern, L. J. Dixon, and D. A. Kosower, *Annu. Rev. Nucl. Part. Sci.* **46**, 109 (1996).
- [13] Z. Bern and A. G. Morgan, *Nucl. Phys.* **B467**, 479 (1996).
- [14] Z. Bern, L. J. Dixon, and D. A. Kosower, *Nucl. Phys.* **B513**, 3 (1998).
- [15] Z. Bern, L. J. Dixon, D. C. Dunbar, and D. A. Kosower, *Phys. Lett. B* **394**, 105 (1997).
- [16] R. Britto, F. Cachazo, and B. Feng, *Nucl. Phys.* **B725**, 275 (2005).
- [17] R. Britto, F. Cachazo, and B. Feng, *Phys. Rev. D* **71**, 025012 (2005); S. J. Bidder, N. E. J. Bjerrum-Bohr, L. J. Dixon, and D. C. Dunbar, *Phys. Lett. B* **606**, 189 (2005); S. J. Bidder, N. E. J. Bjerrum-Bohr, D. C. Dunbar, and W. B. Perkins, *Phys. Lett. B* **612**, 75 (2005); S. J. Bidder, D. C. Dunbar, and W. B. Perkins, *J. High Energy Phys.* **08** (2005) 055; Z. Bern, N. E. J. Bjerrum-Bohr, D. C. Dunbar, and H. Ita, *J. High Energy Phys.* **11** (2005) 027; N. E. J. Bjerrum-Bohr, D. C. Dunbar, and W. B. Perkins, *J. High Energy Phys.* **04** (2008) 038.
- [18] Z. Bern, L. J. Dixon, and D. A. Kosower, *Phys. Rev. D* **73**, 065013 (2006).
- [19] R. Britto, E. Buchbinder, F. Cachazo, and B. Feng, *Phys. Rev. D* **72**, 065012 (2005); R. Britto, B. Feng, and P. Mastrolia, *Phys. Rev. D* **73**, 105004 (2006); P. Mastrolia, *Phys. Lett. B* **644**, 272 (2007).
- [20] A. Brandhuber, S. McNamara, B. J. Spence, and G. Travaglini, *J. High Energy Phys.* **10** (2005) 011.
- [21] G. Ossola, C. G. Papadopoulos, and R. Pittau, *Nucl. Phys.* **B763**, 147 (2007).
- [22] Z. Bern, L. J. Dixon, and D. A. Kosower, *Ann. Phys. (Amsterdam)* **322**, 1587 (2007).
- [23] D. Forde, *Phys. Rev. D* **75**, 125019 (2007).
- [24] S. D. Badger, *J. High Energy Phys.* **01** (2009) 049.
- [25] C. Anastasiou, R. Britto, B. Feng, Z. Kunszt, and P. Mastrolia, *Phys. Lett. B* **645**, 213 (2007); *J. High Energy Phys.* **03** (2007) 111; W. T. Giele, Z. Kunszt, and K. Melnikov, *J. High Energy Phys.* **04** (2008) 049.
- [26] R. Britto and B. Feng, *Phys. Rev. D* **75**, 105006 (2007); *J. High Energy Phys.* **02** (2008) 095; R. Britto, B. Feng, and G. Yang, *J. High Energy Phys.* **09** (2008) 089. R. Britto, B. Feng, and P. Mastrolia, *Phys. Rev. D* **78**, 025031 (2008).
- [27] C. F. Berger and D. Forde, *Annu. Rev. Nucl. Part. Sci.* **60**, 181 (2010).
- [28] Z. Bern, J. J. Carrasco, T. Dennen, Y. T. Huang, and H. Ita, *Phys. Rev. D* **83**, 085022 (2011).
- [29] H. Elvang and Y.-t. Huang, [arXiv:1308.1697](https://arxiv.org/abs/1308.1697).
- [30] R. K. Ellis, W. T. Giele, and Z. Kunszt, *J. High Energy Phys.* **03** (2008) 003.
- [31] C. F. Berger, Z. Bern, L. J. Dixon, F. Febres Cordero, D. Forde, H. Ita, D. A. Kosower, and D. Maître, *Phys. Rev. D* **78**, 036003 (2008).
- [32] G. Ossola, C. G. Papadopoulos, and R. Pittau, *J. High Energy Phys.* **03** (2008) 042.
- [33] P. Mastrolia, G. Ossola, C. G. Papadopoulos, and R. Pittau, *J. High Energy Phys.* **06** (2008) 030.
- [34] W. T. Giele and G. Zanderighi, *J. High Energy Phys.* **06** (2008) 038; R. K. Ellis, W. T. Giele, Z. Kunszt, K. Melnikov, and G. Zanderighi, *J. High Energy Phys.* **01** (2009) 012.
- [35] C. F. Berger, Z. Bern, L. J. Dixon, F. Febres Cordero, D. Forde, T. Gleisberg, H. Ita, D. A. Kosower, and D. Maître, *Phys. Rev. Lett.* **102**, 222001 (2009).
- [36] G. Bevilacqua, M. Czakon, C. G. Papadopoulos, R. Pittau, and M. Worek, *J. High Energy Phys.* **09** (2009) 109.
- [37] P. Mastrolia, G. Ossola, T. Reiter, and F. Tramontano, *J. High Energy Phys.* **08** (2010) 080.
- [38] C. F. Berger, Z. Bern, L. J. Dixon, F. Febres Cordero, D. Forde, T. Gleisberg, H. Ita, D. A. Kosower, and D. Maître, *Phys. Rev. Lett.* **106**, 092001 (2011).
- [39] S. Badger, B. Biedermann, and P. Uwer, *Comput. Phys. Commun.* **182**, 1674 (2011).
- [40] V. Hirschi, R. Frederix, S. Frixione, M. V. Garzelli, F. Maltoni, and R. Pittau, *J. High Energy Phys.* **05** (2011) 044.
- [41] P. Mastrolia and G. Ossola, *J. High Energy Phys.* **11** (2011) 014.
- [42] S. Badger, H. Frellesvig, and Y. Zhang, *J. High Energy Phys.* **04** (2012) 055; **08** (2012) 065.
- [43] Y. Zhang, *J. High Energy Phys.* **09** (2012) 042.
- [44] P. Mastrolia, E. Mirabella, G. Ossola, and T. Peraro, *Phys. Lett. B* **718**, 173 (2012).
- [45] R. H. P. Kleiss, I. Malamos, C. G. Papadopoulos, and R. Verheyen, *J. High Energy Phys.* **12** (2012) 038.
- [46] P. Mastrolia, E. Mirabella, G. Ossola, and T. Peraro, *Phys. Rev. D* **87**, 085026 (2013).
- [47] P. Mastrolia, E. Mirabella, G. Ossola, T. Peraro, and H. van Deurzen, *Proc. Sci.*, LL2012 (2012) 028 [[arXiv:1209.5678](https://arxiv.org/abs/1209.5678)].
- [48] R. Huang and Y. Zhang, *J. High Energy Phys.* **04** (2013) 080.
- [49] P. Mastrolia, E. Mirabella, G. Ossola, and T. Peraro, *Phys. Lett. B* **727**, 532 (2013).
- [50] N. Arkani-Hamed, F. Cachazo, C. Cheung, and J. Kaplan, *J. High Energy Phys.* **03** (2010) 020.
- [51] N. Arkani-Hamed, J. Bourjaily, F. Cachazo, and J. Trnka, *J. High Energy Phys.* **01** (2011) 049.
- [52] N. Arkani-Hamed, J. L. Bourjaily, F. Cachazo, S. Caron-Huot, and J. Trnka, *J. High Energy Phys.* **01** (2011) 041.
- [53] N. Arkani-Hamed, J. L. Bourjaily, F. Cachazo, A. Hodges, and J. Trnka, *J. High Energy Phys.* **04** (2012) 081.
- [54] N. Arkani-Hamed, J. L. Bourjaily, F. Cachazo, and J. Trnka, *J. High Energy Phys.* **06** (2012) 125.
- [55] N. Arkani-Hamed, J. L. Bourjaily, F. Cachazo, A. B. Goncharov, A. Postnikov, and J. Trnka, [arXiv:1212.5605](https://arxiv.org/abs/1212.5605).
- [56] B. Feng and R. Huang, *J. High Energy Phys.* **02** (2013) 117.
- [57] Z. Bern, J. S. Rozowsky, and B. Yan, *Phys. Lett. B* **401**, 273 (1997).

- [58] C. Anastasiou, Z. Bern, L. J. Dixon, and D. A. Kosower, *Phys. Rev. Lett.* **91**, 251602 (2003).
- [59] Z. Bern, L. J. Dixon, and V. A. Smirnov, *Phys. Rev. D* **72**, 085001 (2005).
- [60] Z. Bern, M. Czakon, D. A. Kosower, R. Roiban, and V. A. Smirnov, *Phys. Rev. Lett.* **97**, 181601 (2006).
- [61] Z. Bern, M. Czakon, L. J. Dixon, D. A. Kosower, and V. A. Smirnov, *Phys. Rev. D* **75**, 085010 (2007).
- [62] Z. Bern, L. J. Dixon, D. A. Kosower, R. Roiban, M. Spradlin, C. Vergu, and A. Volovich, *Phys. Rev. D* **78**, 045007 (2008).
- [63] D. A. Kosower, R. Roiban, and C. Vergu, *Phys. Rev. D* **83**, 065018 (2011).
- [64] Z. Bern, C. Boucher-Veronneau, and H. Johansson, *Phys. Rev. D* **84**, 105035 (2011).
- [65] Z. Bern, L. J. Dixon, and D. A. Kosower, *J. High Energy Phys.* **01** (2000) 027.
- [66] Z. Bern, A. De Freitas, and L. J. Dixon, *J. High Energy Phys.* **03** (2002) 018.
- [67] Z. Bern, A. De Freitas, and L. J. Dixon, *J. High Energy Phys.* **09** (2001) 037.
- [68] Z. Bern, A. De Freitas, L. J. Dixon, and H. L. Wong, *Phys. Rev. D* **66**, 085002 (2002).
- [69] Z. Bern, A. De Freitas, and L. J. Dixon, *J. High Energy Phys.* **06** (2003) 028.
- [70] Z. Bern, L. J. Dixon, and D. A. Kosower, *J. High Energy Phys.* **08** (2004) 012.
- [71] A. De Freitas and Z. Bern, *J. High Energy Phys.* **09** (2004) 039.
- [72] Z. Bern, J. J. M. Carrasco, H. Johansson, and D. A. Kosower, *Phys. Rev. D* **76**, 125020 (2007).
- [73] Z. Bern, J. J. M. Carrasco, L. J. Dixon, H. Johansson, and R. Roiban, *Phys. Rev. D* **78**, 105019 (2008).
- [74] F. Cachazo, [arXiv:0803.1988](https://arxiv.org/abs/0803.1988); F. Cachazo, M. Spradlin, and A. Volovich, *Phys. Rev. D* **78**, 105022 (2008).
- [75] Z. Bern, J. J. M. Carrasco, L. J. Dixon, H. Johansson, and R. Roiban, *Phys. Rev. D* **82**, 125040 (2010).
- [76] J. J. M. Carrasco and H. Johansson, *J. Phys. A* **44**, 454004 (2011).
- [77] J. J. M. Carrasco and H. Johansson, *Phys. Rev. D* **85**, 025006 (2012).
- [78] Z. Bern, J. J. M. Carrasco, H. Johansson, and R. Roiban, *Phys. Rev. Lett.* **109**, 241602 (2012).
- [79] D. A. Kosower and K. J. Larsen, *Phys. Rev. D* **85**, 045017 (2012).
- [80] H. Johansson, D. A. Kosower, and K. J. Larsen, *Phys. Rev. D* **87**, 025030 (2013).
- [81] H. Johansson, D. A. Kosower, and K. J. Larsen, *Proc. Sci.*, LL2012 (2012) 066 [[arXiv:1212.2132](https://arxiv.org/abs/1212.2132)].
- [82] S. Caron-Huot and K. J. Larsen, *J. High Energy Phys.* **10** (2012) 026.
- [83] J. Gluza, K. Kajda, and D. A. Kosower, *Phys. Rev. D* **83**, 045012 (2011).
- [84] J. M. Henn, *Phys. Rev. Lett.* **110**, 251601 (2013).
- [85] J. M. Henn, A. V. Smirnov, and V. A. Smirnov, *J. High Energy Phys.* **07** (2013) 128.
- [86] J. M. Henn and V. A. Smirnov, *J. High Energy Phys.* **11** (2013) 041.
- [87] M. SØgaard, *J. High Energy Phys.* **09** (2013) 116.
- [88] F. V. Tkachov, *Phys. Lett.* **100B**, 65 (1981); K. G. Chetyrkin and F. V. Tkachov, *Nucl. Phys.* **B192**, 159 (1981).
- [89] S. Laporta, *Phys. Lett. B* **504**, 188 (2001); *Int. J. Mod. Phys. A* **15**, 5087 (2000).
- [90] T. Gehrmann and E. Remiddi, *Nucl. Phys.* **B580**, 485 (2000).
- [91] R. N. Lee, *J. High Energy Phys.* **07** (2008) 031.
- [92] C. Anastasiou and A. Lazopoulos, *J. High Energy Phys.* **07** (2004) 046.
- [93] A. V. Smirnov, *J. High Energy Phys.* **10** (2008) 107.
- [94] C. Studerus, *Comput. Phys. Commun.* **181**, 1293 (2010).
- [95] A. V. Smirnov and A. V. Petukhov, *Lett. Math. Phys.* **97**, 37 (2011).
- [96] R. Roiban, M. Spradlin, and A. Volovich, *Phys. Rev. D* **70**, 026009 (2004).
- [97] C. Vergu, *Phys. Rev. D* **75**, 025028 (2007).
- [98] L. J. Mason and D. Skinner, *J. High Energy Phys.* **01** (2010) 064; **12** (2010) 018.